Radiation Dose Measurements of the Insertion Devices Using Radiachromic Film Dosimeters

J. Alderman, E. Semones, and P.K. Job
APS Operations Division
Advanced Photon Source

February 9, 2004

Table of Contents

Introduction

The Advanced Photon Source (APS) uses Nd-Fe-B permanent magnets in the insertion devices to produce x-rays for scientific research [1,2]. Earlier investigations have exhibited varying degrees of demagnetization of these magnets [3] due to irradiation from electron beams [4,5,6], ^{60}Co γ-rays [5], and high-energy neutrons [7,8]. Radiation-induced demagnetization has been observed in the APS insertion devices [9] and was first measured in December of 2001. Partial demagnetization has also been observed in insertion devices at the European Synchrotron Radiation Facility (ESRF) [4,6], where Nd-Fe-B permanent magnets are also used. Growing concern for the lifetime of APS insertion devices, as well as the permanent magnets that will be used in next-generation, high-power light sources, like the FEL [10,11], resulted from the partial demagnetization observations made at both facilities. This concern in relation to radiation-induced demagnetization spurred a long-term project to measure and analyze the absorbed doses received by the APS insertion devices. The project required a reliable photon high-dose dosimetry technique capable of measuring absorbed doses greater than 10^6 rad, which was not readily available at the APS. Through a collaboration with the National Institute of Standards and Technology (NIST), one such technique using radiachromic films was considered, tested, and calibrated at the APS. This consequently led to the implementation of radiachromic film dosimetry for measuring the absorbed doses received by the insertion devices for each of the APS runs.

Radiachromic Film Dosimeters

Radiachromic film dosimeters are nylon-based aminotriphenyl methane dye derivatives [12,13]. Upon exposure to ultraviolet light or ionizing radiation, these films undergo radiation-induced coloration by photoionization [12,14]. The photochemical reaction that takes place when the radiachromic films are exposed to ultraviolet light or ionizing radiation is displayed in Figure 1. The change from a clear or colorless state to a deep blue-colored state occurs gradually as a direct function of the radiation exposure received [12,15]. The change in the color intensity, or optical density, is measured using a radiachromic reader, or simple spectrophotometer. The radiachromic films used at the APS have a linear response to ionizing radiation over a dose range of approximately 0.1 Mrad to 20 Mrad [12,15,16]. They have an equivalent response to x-rays, γ-rays, and electrons from ultraviolet energies up to approximately 10 MeV [17,18,19]. Radiachromic films also have a dose rate independence to over 10^{14} rads/s [12].

Radiachromic films were specifically designed for radiation processing quality control, so they are rugged and easy to handle. At the APS, these films are first placed inside small detector envelopes and then placed inside aluminized Mylar envelopes to protect them from ultraviolet exposure [15] and mechanical damage. The nylon-based material used in radiachromic films exhibits few or no environmental affects [12]. The films displayed a constant response for exposures in air and vacuum, as well as in the presence of ozone [12,13,20]. These stable conditions, along with simple handling procedures and no temperature dependence up to 50°C [15], led to the implementation of radiachromic film dosimetry for measuring the absorbed doses received by the APS insertion devices.

A lab has been set up at the APS for radiachromic film processing. A PC-based radiachromic film reader, along with the associated software, was procured from Far West Technology of Goleta, California. Two different types of films were procured including FWT-60 radiachromic films procured from Far West Technology and HD-810 GafChromic films procured from ISP Technologies, Inc., of Wayne, New Jersey. The HD-810 GafChromic films are special films that are useful for measuring doses outside the storage ring, where absorbed doses are typically in the kilorad range. FWT-60 radiachromic films used at the APS can be used to measure absorbed doses up to approximately 20 Mrad.

Calibration

A collaboration was formed with NIST to calibrate the FWT-60 radiachromic films and the HD-810 GafChromic films. The NIST standard gamma irradiation facility GC232 was used to calibrate the FWT-60 films, and the GC45 facility was used to calibrate the HD-810 films. The relative humidity was maintained at 44% during irradiation. The individual films were first placed inside paper detector envelopes and then sealed in aluminized Mylar pouches. During irradiation, the pouches were placed between two 5.0-mm-thick blocks of polystyrene, in order to simulate tissue absorption, and were held upright on the polystyrene pedestal. The temperature during irradiation was controlled with forced air blown down onto the samples and measured every sixty seconds. The

irradiation dose rate for the FWT-60 radiachromic films was 936.3 krad/h. The irradiation dose rate for the HD-810 GafChromic films was 283.8 krad/h. The FWT-60 radiachromic films were calibrated up to 20.0 Mrad. The HD-810 GafChromic films were calibrated up to 0.20 Mrad.

A calibration check of the FWT-60 radiachromic films was performed in late 2002 and displayed very little change as compared to the initial calibration performed in 1998. A graphic comparison of the two calibration curves up to a dose of 20 Mrad is given in Figure 2.

Radiachromic Film Placement

During the period of time that encompassed the APS runs during 1996 and 1997, up to six radiachromic films were placed on and around each insertion device. The films were placed above and below the vacuum chamber at locations upstream and downstream of the insertion device. The films were also placed directly on the upstream and downstream end of the upper magnetic structure of the insertion device. After two years, the data were analyzed, and placement of the radiachromic films directly on the upstream and downstream end of the upper magnetic structure of the insertion device was determined to be ideal for the measurement of the absorbed doses received by the insertion devices. As a result, after 1998-1 only two radiachromic films were placed on each insertion device during any given run. The current placement location of the radiachromic films on and around the insertion devices is given in Figure 3.

For two runs in 1999 four radiachromic films were placed on each insertion device. Along with the two radiachromic films that were normally placed on the upstream and downstream end of the upper magnetic structure, two radiachromic films were placed on the upstream and downstream end of the lower magnetic structure. This was done to determine if there was a difference between the absorbed doses received by the upper magnetic structures of the insertion devices as compared to the lower magnetic structures of the insertion devices. The extra radiachromic films were used for two runs in 1999. The difference between the absorbed doses received by the upper magnetic structures as compared to the lower magnetic structures, displayed in Figure 4, was insignificant. Subsequently it was decided that it was sufficient to place two radiachromic films on each insertion device. The radiachromic dosimeters are placed on each insertion device at the beginning of every run and left in place for the duration of the run.

Statistics for every run are recorded so that cumulative absorbed doses per sector can be normalized according to total Amp-h. Table 1 gives the run statistics for all of the runs beginning with Run 1996-6. The locations of insertion devices are also recorded in order to keep track of the movement of insertion devices to different sectors, and the fact that, for some runs, two insertion devices are used in one sector. This allows for an accurate accumulation of the total absorbed doses received by each individual insertion device, as well as the total absorbed doses received per sector.

Results and Discussion

a. Doses Received by the Insertion Devices
Following every run, the radiachromic films are retrieved from the storage ring, and the optical density changes are analyzed using the radiachromic film reader. Measured insertion device doses can then be determined from the changes in optical density using the calibration curve and associated calibration equation. The measured insertion device doses received during each run from Run 1996-6 to Run 2003-3 are given in Figures 5-35.

Broad observations can initially be drawn from the measured insertion device doses received during each run. It is evident from the data provided in Figures 5-35 that random fluctuations in dose occur from run to run. Just because the dose received by a particular device was higher than normal in one run does not mean that it will be abnormally higher in the next run. Another observation is that the typical dose received by an APS insertion device is usually less than 1E+06 rad per run. This is particularly evident in Figure 18, which gives the measured insertion device doses for Run 1999-1 and Run 1999-2 combined. Figure 18 also exhibits a maximum dose of 1.9E+06 rad received by an insertion device during a particular run. Displaying the data in terms of the dose received by each insertion device provides a general picture of the overall dose distribution and allows general conclusions to be drawn.

We are ultimately interested in the total doses received by each insertion device in relation to radiation-induced demagnetization of the insertion devices over time. Therefore it is important to look at the data in terms of the cumulative doses received by each device. The use of radiachromic films for the measurement of absorbed doses received by the APS insertion devices began with the last run in 1996, Run 1996-6. All of the data beginning with Run 1996-6 and ending with Run 2003-3 have been compiled to exhibit the total doses received by each of the APS insertion devices over a seven-year period. The cumulative insertion device doses for Run 1996-6 to Run 2003-3 are given in Figure 36. These total doses take into account the occasional movement of the insertion devices and provide the total dose to the device itself, regardless of location in the storage ring. As of Run 1996-6, radiachromic films have been placed on every insertion device as they are installed, and the films are retrieved and replaced with new films after every run.

Figure 36 shows that the highest cumulative insertion device dose over the seven-year period beginning with Run 1996-6 and ending with Run 2003-3 was approximately 6.3E+07 rad. This "worst case" dose rate of 6.3E+07 rad every seven years can be projected to determine the approximate cumulative absorbed dose received in a twenty-year period, which is the desired lifespan of the insertion devices. In other words, a dose rate of 6.3E+07 rad every seven years would give approximately 1.8E+08 rad after twenty years as a projected dose estimate.

b. Radiachromic Films as Beam Loss Monitors
Radiachromic films can also act as passive beam loss monitors that provide information concerning the average beam loss per sector, per run. The data are arranged according to

the absorbed doses received per sector rather than per insertion device. This results in an overall representation of beam loss in each sector, where the higher the absorbed dose in a sector, the greater the beam loss in that particular sector. Figures 37 and 38 provide examples of abnormal beam losses that occurred during Run 1999-1 / 1999-2 and Run 2000-3. In Figure 37 two abnormal beam losses are evident, one in sector 2 and the other in sector 34. The figure shows a greater than average dose in these two sectors for the 1999-1 / 1999-2 run. It is important to point out that the abnormal beam losses could be the result of any number of things. In this particular case, the abnormal beam loss in sector 2 that resulted in a downstream absorbed dose of approximately 1.9E+06 rad could be the result of that particular insertion device being one of two insertion devices placed in sector 2 during the run. When two insertion devices are used in one sector, the upstream device is placed very close to the transition piece, and there is not enough room for the shielding between the transition piece and the insertion device that is usually used. The abnormal beam loss could also be the result of poor beam lifetime, shifting of the insertion device, beam steering, or other machine controls.

A greater than average dose is also evident in sector 34 for the 1999-1 / 1999-2 run. One possible reason for the 1.7E+06 rad absorbed dose on the downstream end of the insertion device could be due to a beam height variation near the device itself. Survey and alignment done in the spring of 1999 observed a beam height variation of +/- 2 mm near sector 34. Beam height variation by this small amount could cause the edge of the insertion device to come into contact with the beam, producing a shower that would result in a greater dose to the insertion device. The abnormal beam loss in sector 34 could also be attributed to beam steering studies that were conducted during Run 1999-1 and Run 1999-2, or any other number of reasons mentioned earlier.

Figure 38 also provides an example of an abnormal beam loss, this one occurring in sector 3 during Run 2000-3. Prior to the third run in 2000, an insertion device vacuum chamber straight section of 5-mm was installed at 3ID in place of the typical 8-mm chamber. A smaller vacuum chamber increases the probability of higher beam losses at the transition piece. Figure 39 shows that the abnormal beam loss is still present during the 2000-4 run, while the 5-mm straight section is still in place. The typical 8-mm straight section was in place for the 2000-2 run shown in Figure 40. As a result, Figure 40 shows that the abnormal beam loss is not present for the 2000-2 run. The evidence of abnormal beam losses present in sector 3 during Run 2000-3 and Run 2000-4 with the 5-mm straight section, as compared to the lack of an abnormal beam loss during Run 2000-2 with the 8-mm straight section, seems to indicate that the smaller vacuum chamber straight section was the cause of the abnormal beam losses present in sector 3 during Run 2000-3 and Run 2000-4.

c. Sector Representation of Doses
Displaying the data in terms of the upstream and downstream doses received in each sector, regardless of the particular insertion device, provides an overall view of the beam loss pattern per sector for each run. Several conclusions can be drawn from sector representation of the data. Comparing Figure 37 and Figure 41, random variation in beam loss evidently occurs from run to run. The abnormal beam loss in sector 2 that is present

in Run 1999-1 and Run 1999-2 is not present in the following run, Run 1999-3. The random variation in beam losses cannot be attributed to one specific cause; they can be attributed to many different factors. Therefore, it is best to discuss the absorbed doses per sector as an average over time.

Sector representation of the radiachromic film data shows that typically the downstream dose is higher than the upstream dose. Figures 37-41 provide a sector-wise comparison of the upstream and downstream doses for several APS runs. Two possible explanations for a typically higher downstream dose are based on the two components of the photon dose present in the APS storage ring. The first possible reason is the result of bremsstrahlung produced from beam losses. The dimensions of the bremsstrahlung shower, produced when the halo of the electron beam strikes the copper transition piece just in front of the insertion device, may not be large enough to strike the insertion device until it reaches the downstream end. The lead shield between the transition piece and the insertion device also shadows or absorbs the bremsstrahlung shower near the upstream end of the insertion device. The second reason that the downstream dose is typically higher than the upstream dose is that synchrotron radiation is much greater in intensity at the downstream end of the insertion device. Although the percentage of scatter off residual gas molecules remains the same throughout the device, a higher absolute number of photons will be scattered at the downstream end because of the greater intensity of synchrotron radiation present. These reasons explain why the downstream absorbed doses are typically higher than the upstream absorbed doses.

As stated before, random variations in beam losses can be attributed to a number of different factors. Therefore it helps to discuss the absorbed doses per sector over time, where devices have been installed, rather than on a run-to-run basis. The measured absorbed doses per sector for each individual run were summed to come up with the measured total sector doses over the seven-year period beginning with Run 1996-6 and ending with Run 2003-3. These doses, given in Figure 42, show that sector 3 received the highest doses during the seven-year period. Interestingly, these high doses of near 5.0E+07 rad 6.0E+07 rad were received in sector 3 as the result of high doses observed in sector three since the end of 2000, or approximately twelve APS runs. In comparison, some sectors, such as sector 11, have had a device in place since the beginning of the seven-year period, a total of 32 APS runs. Yet the cumulative dose for that particular sector is one of the lowest, aside from sectors where devices have been only recently installed. By normalizing the total sector doses with the total number of Amp-h for each run, measured total sector doses are represented regardless of variations in beam current and run times. Figure 43 gives the normalized cumulative sector doses from Run 1996-6 to Run 2003-3, which allows for a representation of the total doses for each sector under the same conditions. The normalized data also provide a clearer representation of the overall total beam loss per sector. Upstream and downstream does for each sector were averaged to provide an average normalized sector dose for each sector where insertion devices have been installed.

Summary and Conclusions

Over the last seven years, beginning with Run 1996-6 and ending with Run 2003-3, radiachromic films have been placed on the APS insertion devices to measure the absorbed doses received by each device during every run. The ideal placement of the radiachromic films to measure the absorbed doses received by each device was determined to be on the upstream and downstream ends of the upper magnetic structure. The difference between the absorbed doses received by the upper magnetic structures of the insertion devices as compared to the doses received by the lower magnetic structures was insignificant. The typical dose received by an APS insertion device is usually less than 1.0E+06 rad/run. However some random fluctuations in dose occur from run to run, and much higher doses have been observed during certain runs.

Radiachromic films act as passive beam loss monitors that provide information regarding beam loss patterns inside the storage ring during each run. In other words, the higher the absorbed dose measured in a particular sector, the greater the beam loss in that sector. Abnormal beam losses, as monitored by radiachromic films, appear to be random and vary from run to run. They usually cannot be attributed to one specific cause. The higher beam losses that were evident in some of the sectors over the years could be explained by poor beam lifetimes, beam steering studies, smaller vacuum chamber dimensions, beam height variations, location of the device within the sector (upstream vs. downstream), and other machine controls.

From the radiachromic film data, it is evident that doses on the downstream end of the insertion devices are typically higher than doses on the upstream end of the devices. This may be explained by the greater amount of synchrotron radiation present, and consequently the higher absolute number of scattered photons at the downstream end of an insertion device. It may also be explained by the greater possibility of a bremsstrahlung shower, produced just in front of the insertion device, to strike the downstream end rather than the upstream end of the insertion device due to the larger dimensions of the shower at the downstream end.

Over the seven-year period beginning with Run 1996-6 and ending with Run 2003-3, the highest dose received by an APS insertion device was approximately 6.3E+07 rad. This worst case scenario is important because we are ultimately interested in the total doses received by each insertion device in relation to the radiation-induced demagnetization of the insertion devices over time. A dose rate of 6.3E+07 rad every seven years could be projected to a dose of 1.8E+08 rad after twenty years, which is the desired lifespan of the insertion devices.

The total sector doses over the seven-year period beginning with Run 1996-6 and ending with Run 2003-3, provide information concerning which sectors, with installed devices, received the highest doses regardless of the specific insertion devices in place, while taking into account the possibility of random variations in beam losses from run to run. Normalizing the total sector doses with the total number of Amp-h for each run takes this one step further and provides information representing the cumulative sector doses

regardless of variations in beam current and run times. This allows for a representation of the total doses for each sector under the same conditions and provides a clearer representation of the overall total beam loss per sector where insertion devices have been installed.

The highest cumulative sector dose received during the seven-year period beginning with Run 1996-6 and ending with Run 2003-3 was near 6.0E+07 rad, measured in sector 3. Consequently, the highest normalized, cumulative sector dose was 0.03E+06 rad/Amp-h in sector 3, compared to an average of 0.001E+06 rad/Amp-h received in all of the other sectors.

References

[1]   The Advanced Photon Source – A National Synchrotron Radiation Research Facility at Argonne National Laboratory, ANL/APS/TB-25-Rev., Argonne National Laboratory, 1997.

[2]   B. Lai, A. Khounsary, R. Savoy, L. Moog, and E. Gluskin, Undulator A Characteristics and Specifications, ANL/APS/TB-3, Argonne National Laboratory, 1993.

[3]   R.D. Brown, and J.R. Cost, Radiation-Induced Changes in Magnetic Properties of Nd-Fe-B Permanent Magnets, *IEEE T. Magn.* 25 (1989) 3117.

[4]   P. Colomp, T. Oddolaye, and P. Ellaeume, Demagnetization of Permanent Magnets to 180 MeV Electron Beam, ESRF/MACH/93-09 (1993).

[5]   S. Okuda, K. Ohashi, and N. Kobayashi, Effects of electron-beam and γ-ray irradiation on the magnetic flux of Nd-Fe-B and Sm-Co permanent magnets, *Nucl. Instrum. Methods B* 94 (1994) 227.

[6]   J. Chavanne, P. Elleaume, and P. Van Vaerenbergh, Partial Demagnetization of ID6 and Dose Measurements on Certain IDs, ESRF Machine Technical Note 1-1996/ID (1996).

[7]   J.R. Cost, R.D. Brown, A.L. Giorgi and J.T. Stanley, Effects of Neutron Irradiation on Nd-Fe-B Magnetic Properties, *IEEE T. Magn.* 24 (1988) 2016.

[8]   R.D. Brown, J.R. Cost, G.P. Meisner, and E.G. Brewer, Neutron irradiation study of Nd-Fe-B permanent magnets made from melt-spun ribbons, *J. Appl. Phys.* 64 (1988) 5305.

[9]   M. Petra, P.K. Den Hartog, E.R. Moog, S. Sasaki, N. Sereno, and I.B. Vasserman, Radiation effects studies at the Advanced Photon Source, *Nucl. Instrum. Methods A* 507 (2003) 422.

[10]   M. Cornacchia et al., Performance and Design Concepts of a Free Electron Laser Operating in the X-ray Region, Presented at LASE97, San Jose, CA (1997).

[11]   A. Fasso, S. Rokni, and V. Vylet, Radiation Studies for a High Energy Free Electron Laser, Proc. of SARE3, Tsukuba, Japan (1997) 233.

[12]   K.C. Humpherys, and A.D. Kantz, Radiachromic: A Radiation Monitoring System, *Radiat. Phys. Chem.* 9 (1977) 737-747.

[13]   K.C. Humpherys, J.D. Rickey, and R.L. Wilcox, Humidity Effects on the Dose Response of Radiachromic Nylon Film Dosimeters, *Radiat. Phys. Chem.* 35 (1990) 713-715.

[14]   J.H. O'Donnell, Chemistry of Radiation Degradation of Polymers, Proc. of ACS Symposium Series 475 (1990) 402.

[15]   W.L. McLaughlin, J.C. Humphreys, D. Hocken, and W.J. Chappas, Radiochromic Dosimetry for Validation and Commissioning of Industrial Radiation Processes, *Radiat. Phys. Chem.* 31 (1988) 505-514.

[16]   W.L. McLaughlin, A. Miller, F. Abdel-Rahim, and T. Preisinger, Plastic Film Materials for Dosimetry of Very Large Absorbed Doses, *Radiat. Phys. Chem.* 25 (1985) 729-748.

[17]   W.L. McLaughlin, National Institute of Standards and Technology, Gaithersburg, MD, Private Communication (1997).

[18]   W.L. McLaughlin, A. Miller, R.M. Uribe, S. Kronenberg, and C.R. Siebentritt, Energy Dependence of Radiochromic Dosimeter Response to X- and γ-Rays, Proc. of an International Symposium on High-Dose Dosimetry, Vienna (1985) 397.

[19]   W.L. McLaughlin, J.C. Humphreys, B.B. Radak, A. Miller, and T.A. Olejnik, The Response of Plastic Dosimeters to Gamma Rays and Electrons at High Absorbed Dose Rates, *Radiat. Phys. Chem.* 14 (1979) 535-550.

[20]   Chen Wenxiu, Jia Haishen, and W.L. McLaughlin, Response of Radiochromic Film Dosimeters to Electron Beams in Different Atmospheres, Proc. of an International Symposium on High-Dose Dosimetry, Vienna (1985) 345.

Table 1: Run Statistics

Run	Amp-h
Run 1996-6	43.7 Amp-h
Run 1996-7	13.2 Amp-h
Run 1997-1	25.2 Amp-h
Run 1997-2	29.3 Amp-h
Run 1997-3	37.4 Amp-h
Run 1997-4	37.2 Amp-h
Run 1997-5	36.2 Amp-h
Run 1997-6	72.4 Amp-h
Run 1997-7	63.0 Amp-h
Run 1998-1	57.2 Amp-h
Run 1998-2	61.0 Amp-h
Run 1998-3	97.4 Amp-h
Run 1998-4	95.0 Amp-h
Run 1998-5	91.3 Amp-h
Run 1999-1	85.6 Amp-h
Run 1999-2	76.0 Amp-h
Run 1999-3	73.3 Amp-h
Run 1999-4	115.7 Amp-h
Run 1999-5	96.6 Amp-h
Run 2000-1	138.8 Amp-h
Run 2000-2	113.1 Amp-h
Run 2000-3	100.7 Amp-h
Run 2000-4	94.1 Amp-h
Run 2001-1	138.7 Amp-h
Run 2001-2	115.7 Amp-h
Run 2001-3	120.2 Amp-h
Run 2001-4	116.3 Amp-h
Run 2002-1	208.6 Amp-h
Run 2002-2	215.7 Amp-h
Run 2002-3	156.9 Amp-h
Run 2003-1	180.2 Amp-h
Run 2003-2	199.7 Amp-h
Run 2003-3	190.8 Amp-h
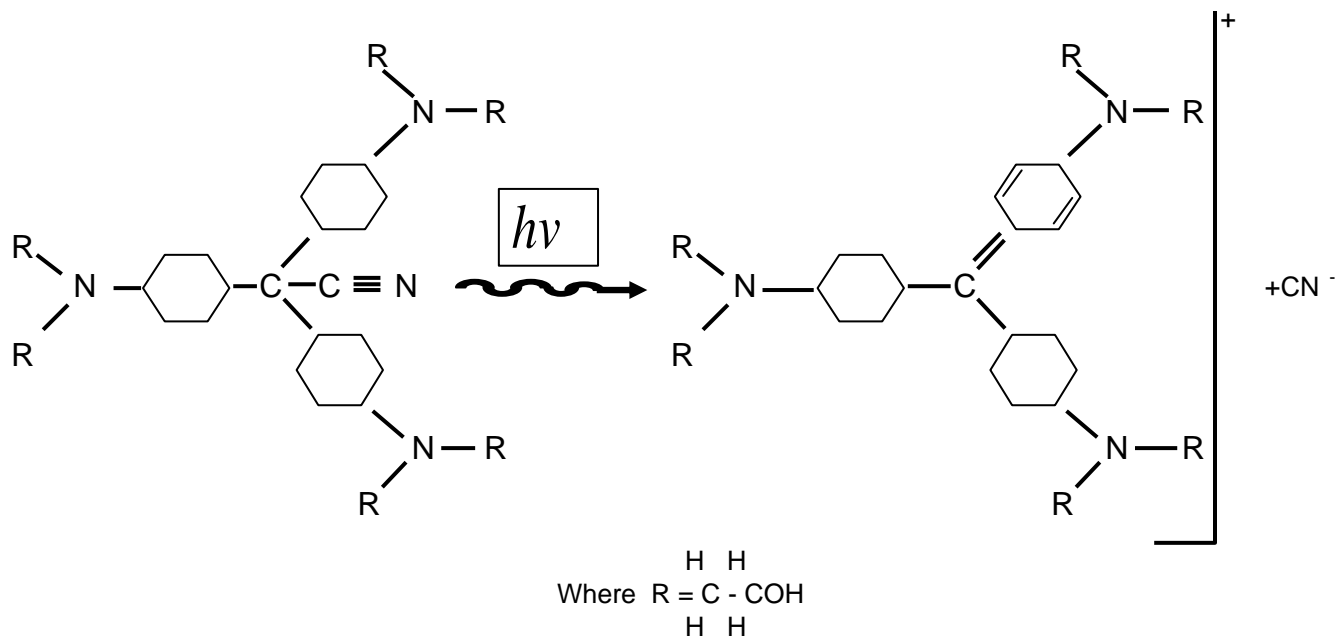
Figure 1: Radiation-Induced Photochemical Reaction
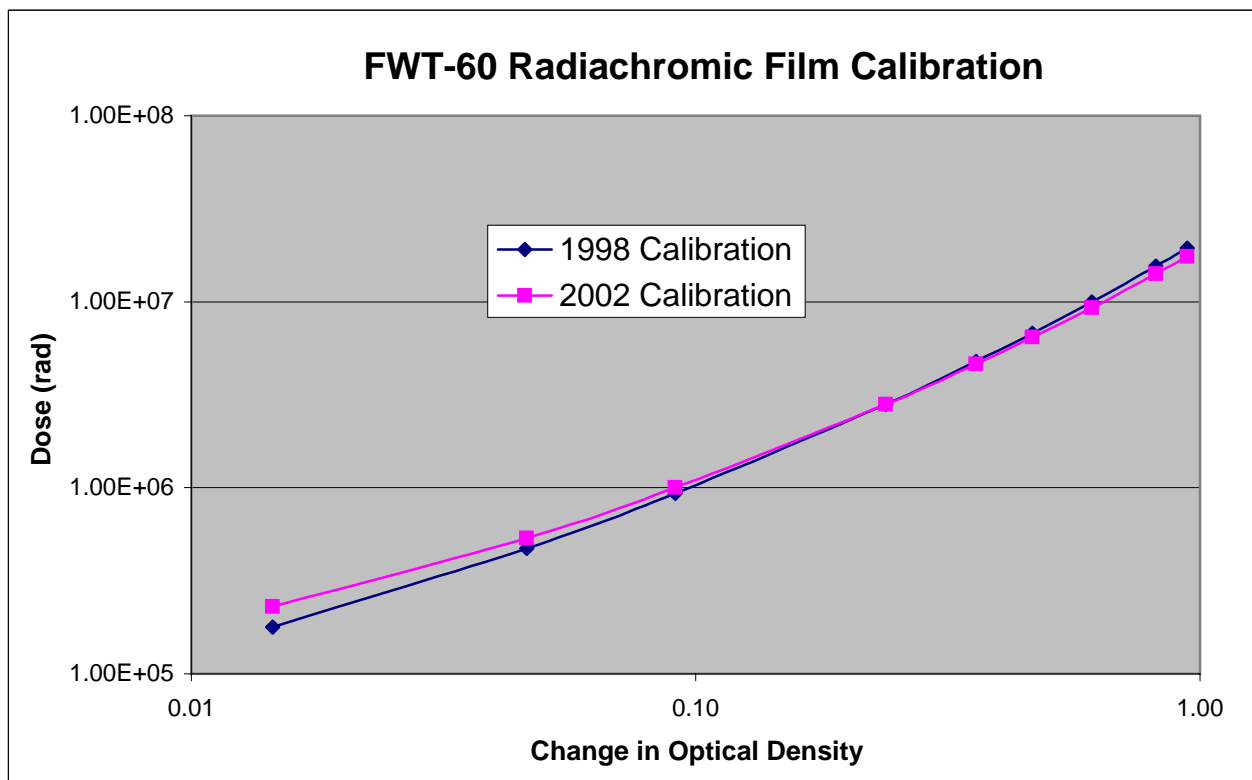
Figure 2: FWT-60 Calibration Curves (1998 and 2002)

11
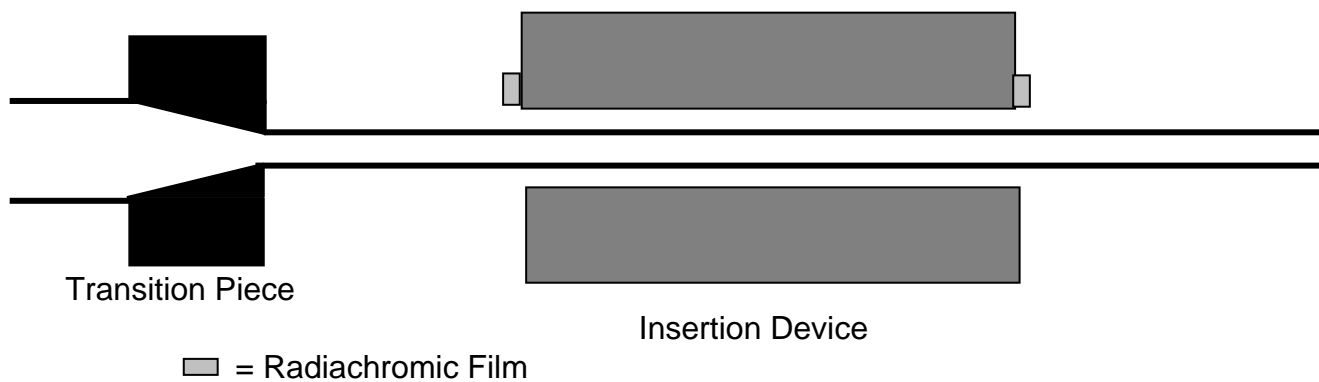
Figure 3: Radiachromic Film Placement
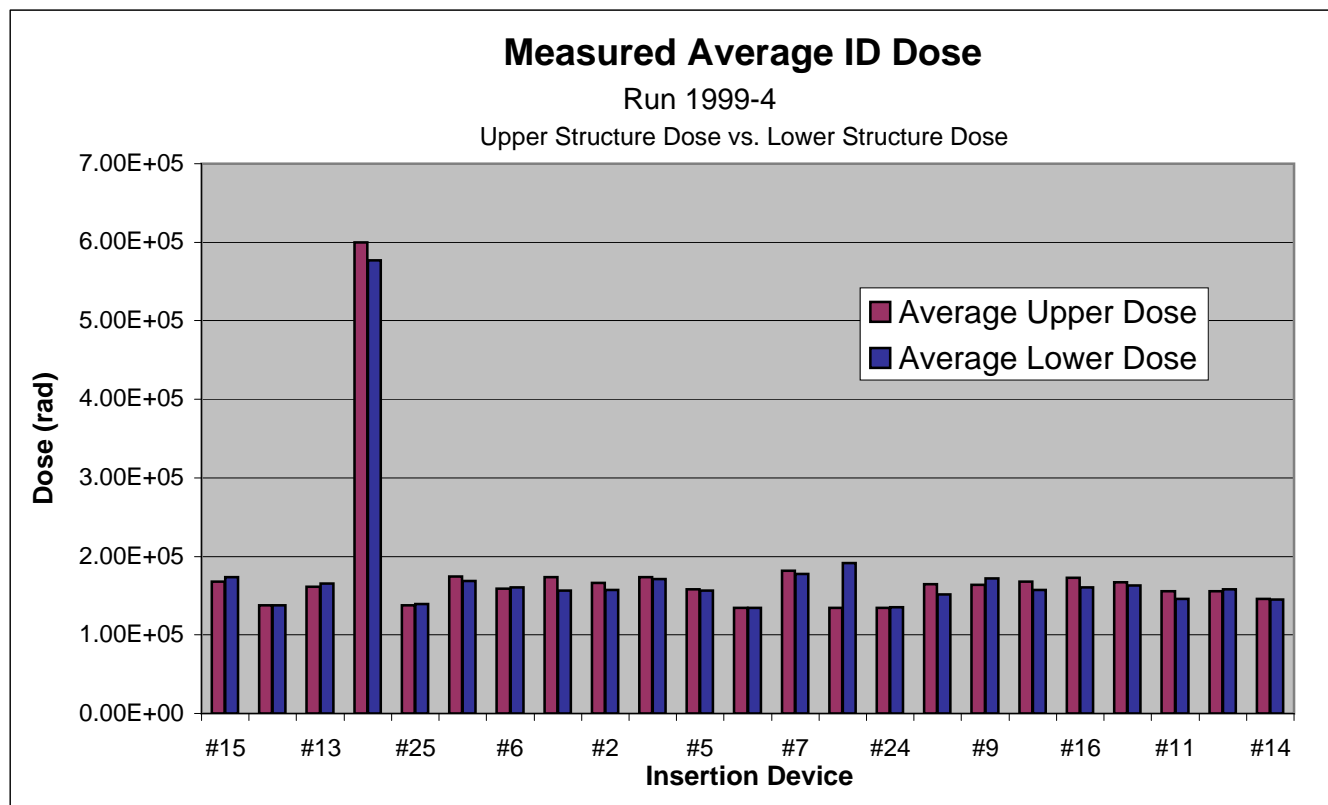
Figure 4: Upper and Lower Structure Dose Comparison
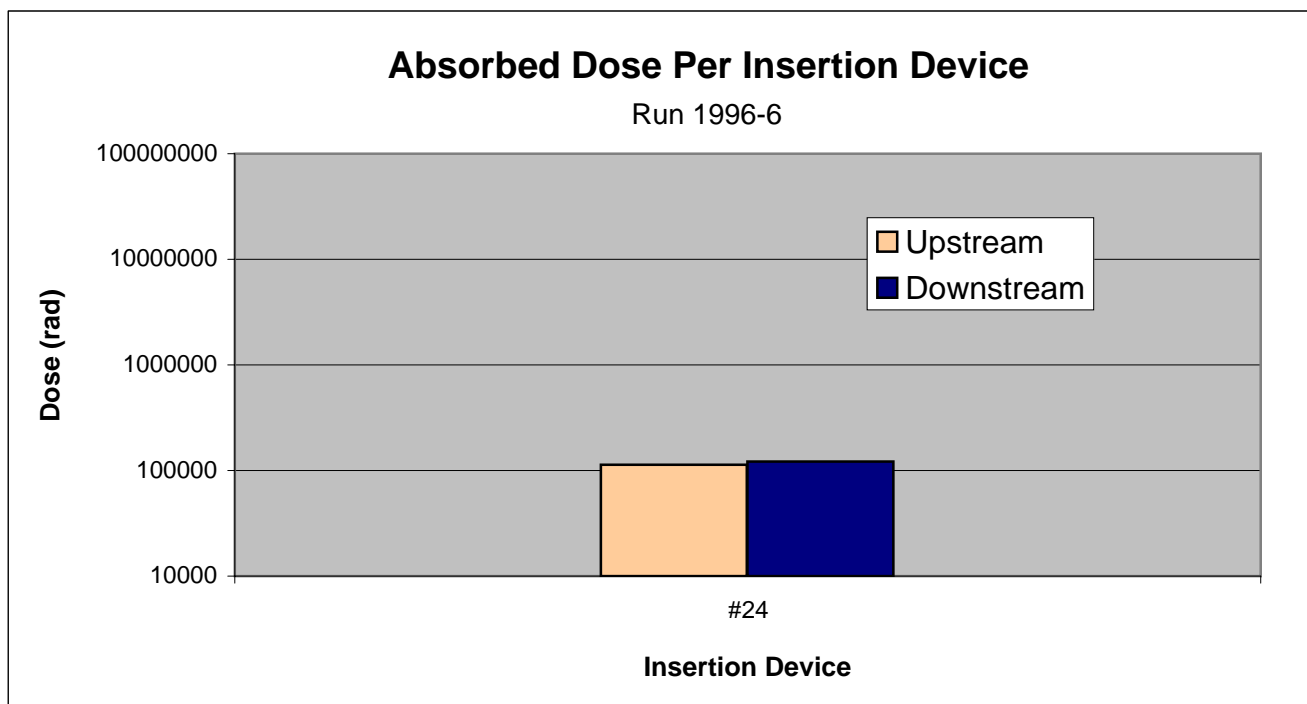
Figure 5: Measured Insertion Device Doses for Run 1996-6
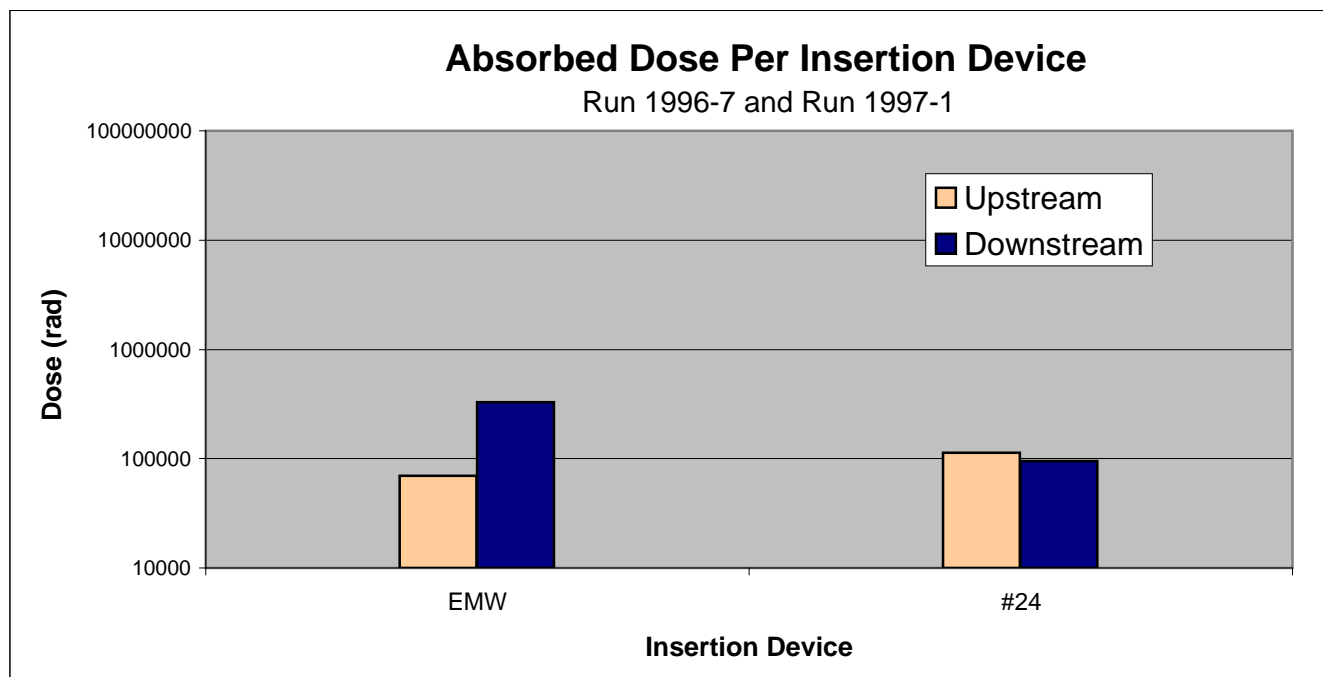
Figure 6: Measured Insertion Device Doses for Run 1996-7 and Run 1997-1
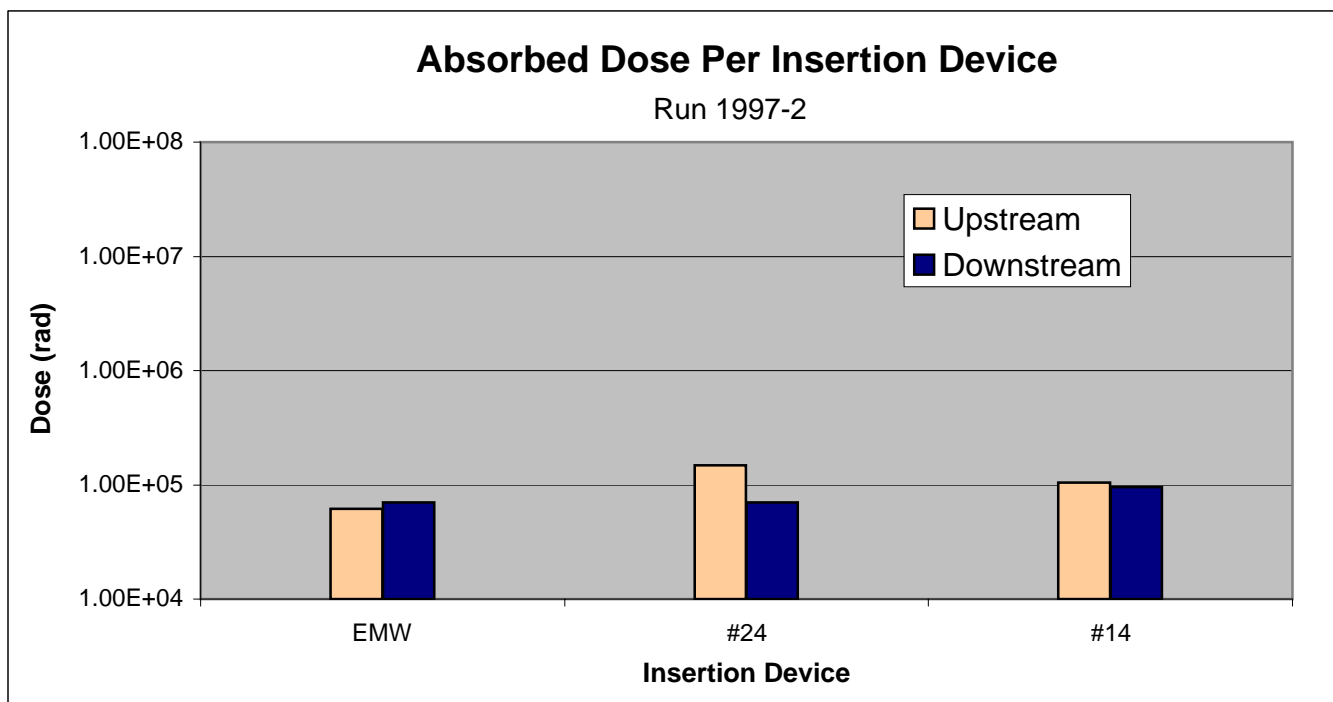
Figure 7: Measured Insertion Device Doses for Run 1997-2
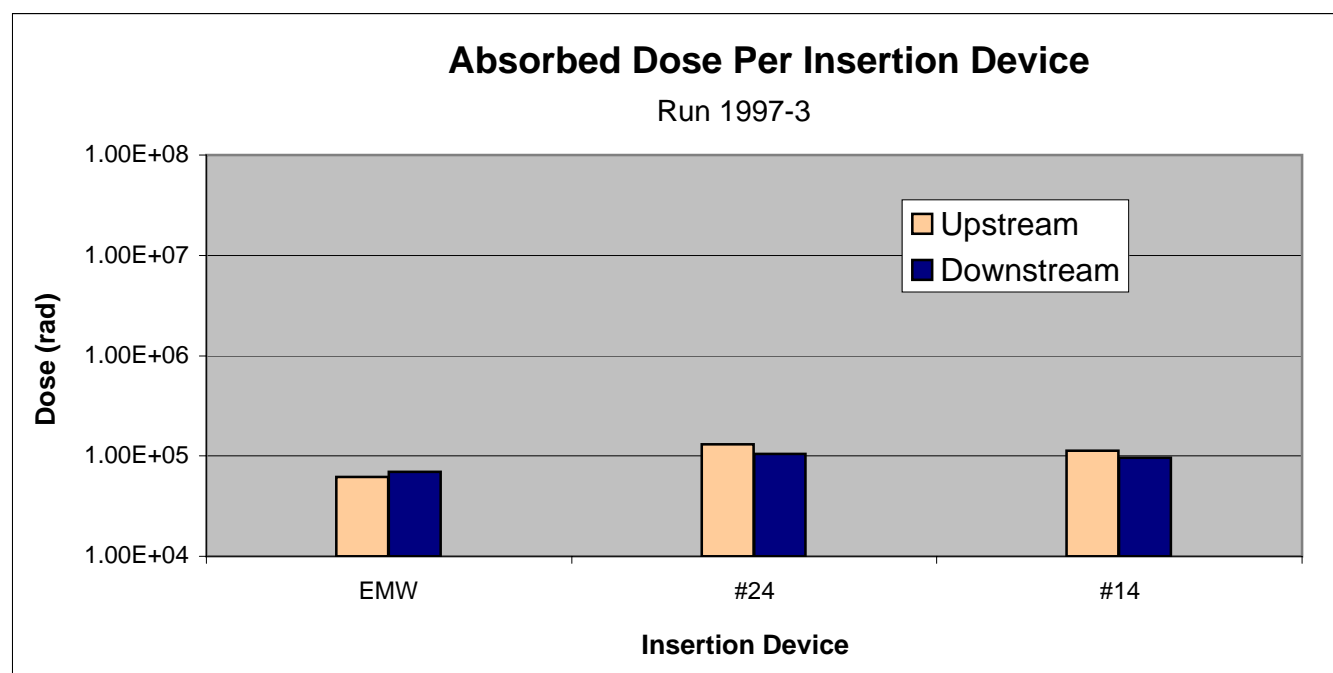
Figure 8: Measured Insertion Device Doses for Run 1997-3
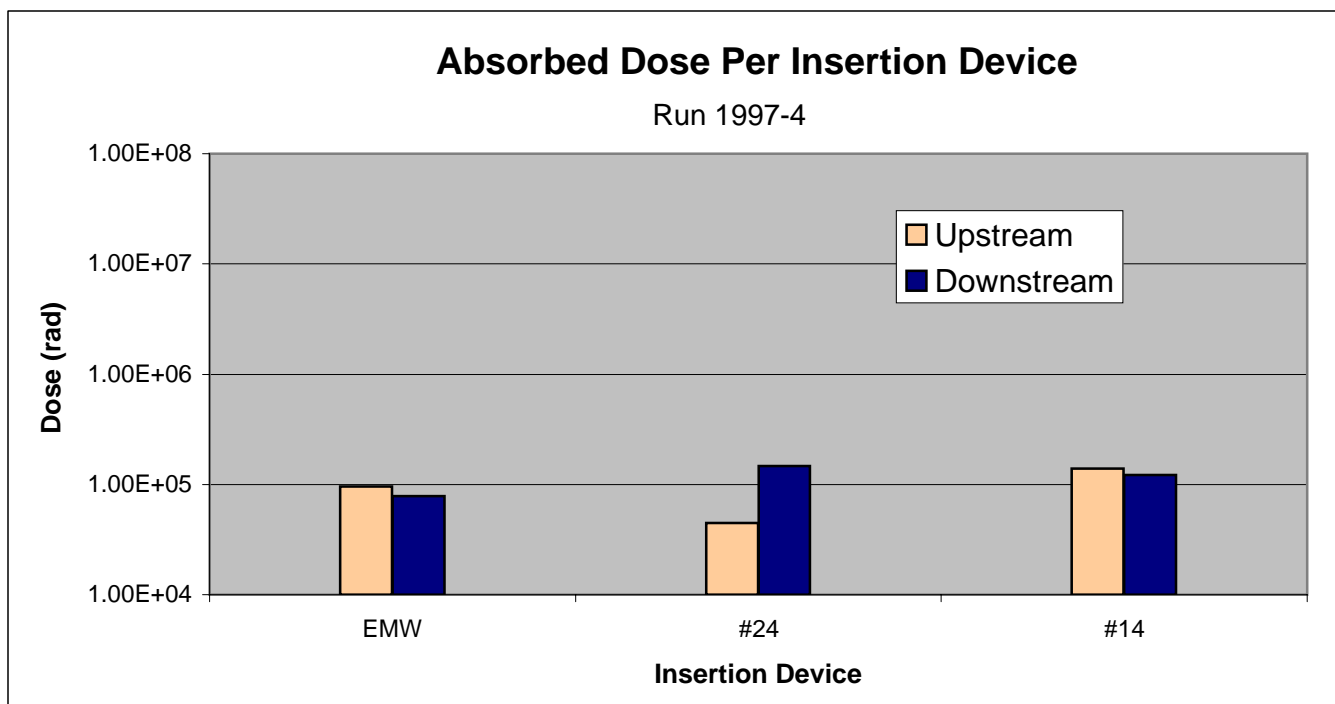
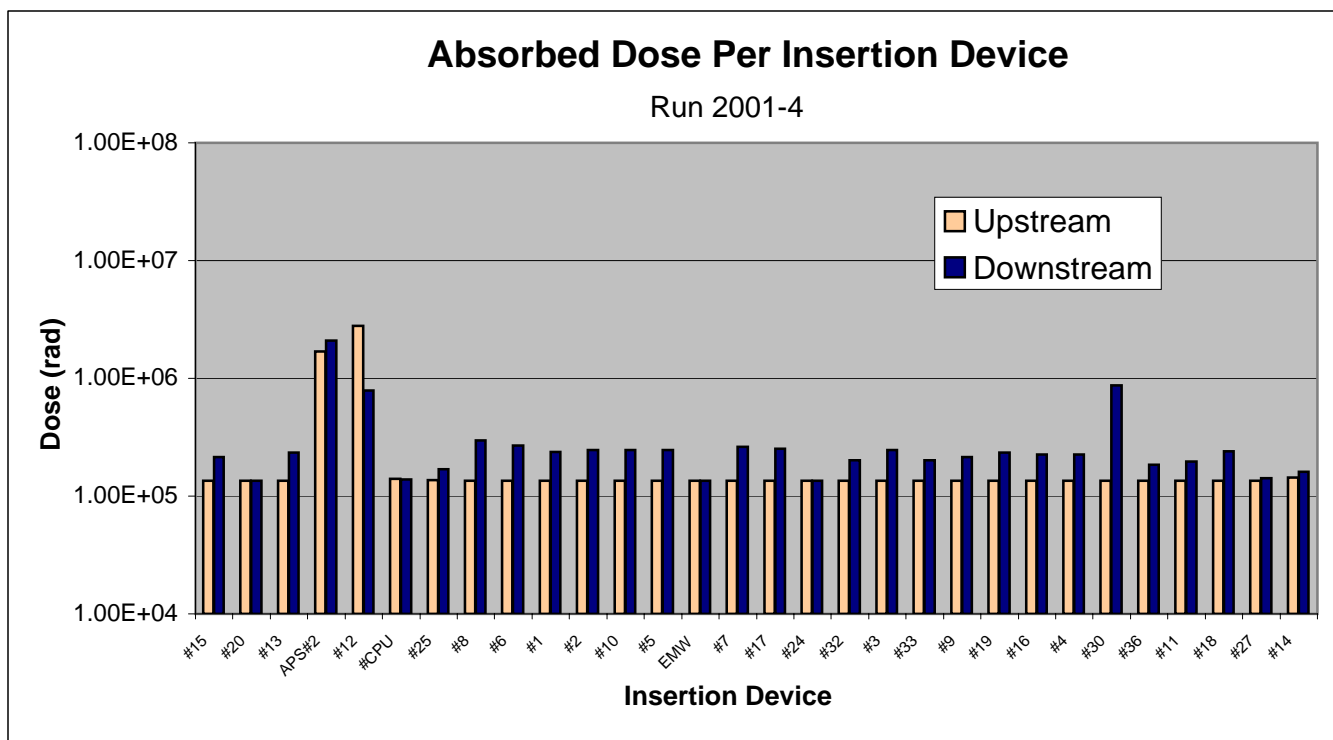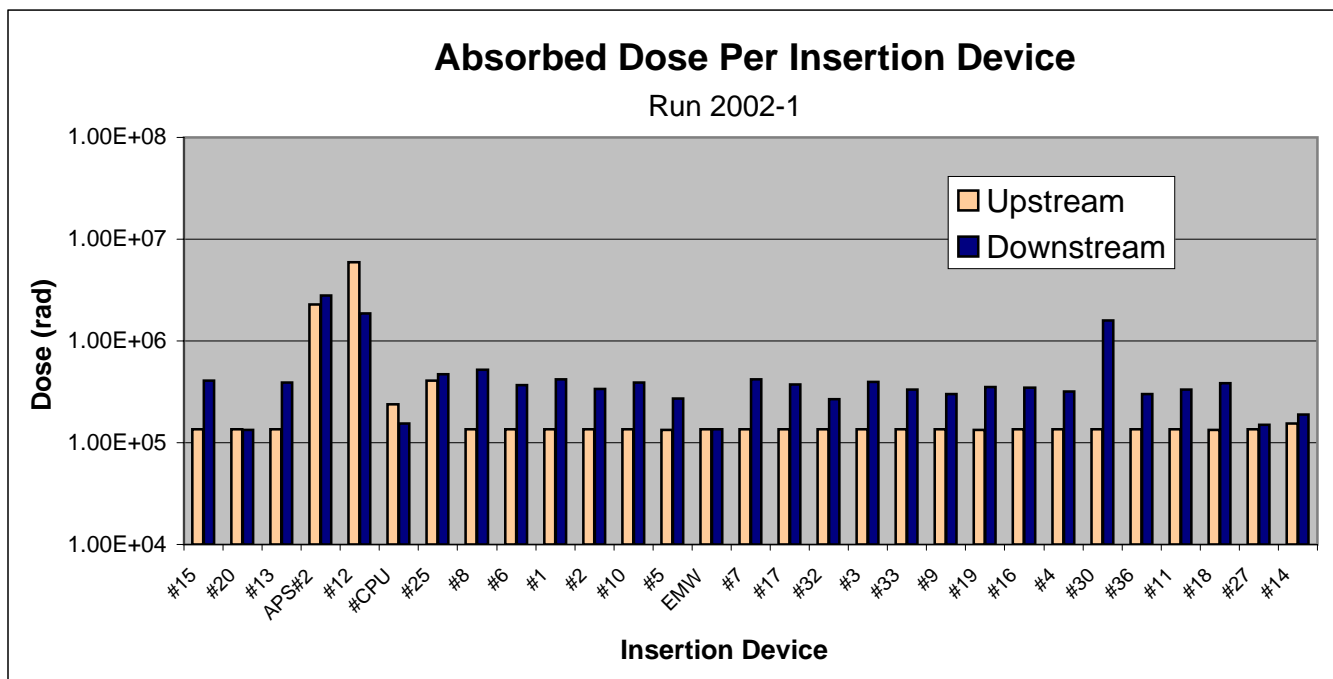**Figure 9: Measured Insertion Device Doses for Run 1997-4**
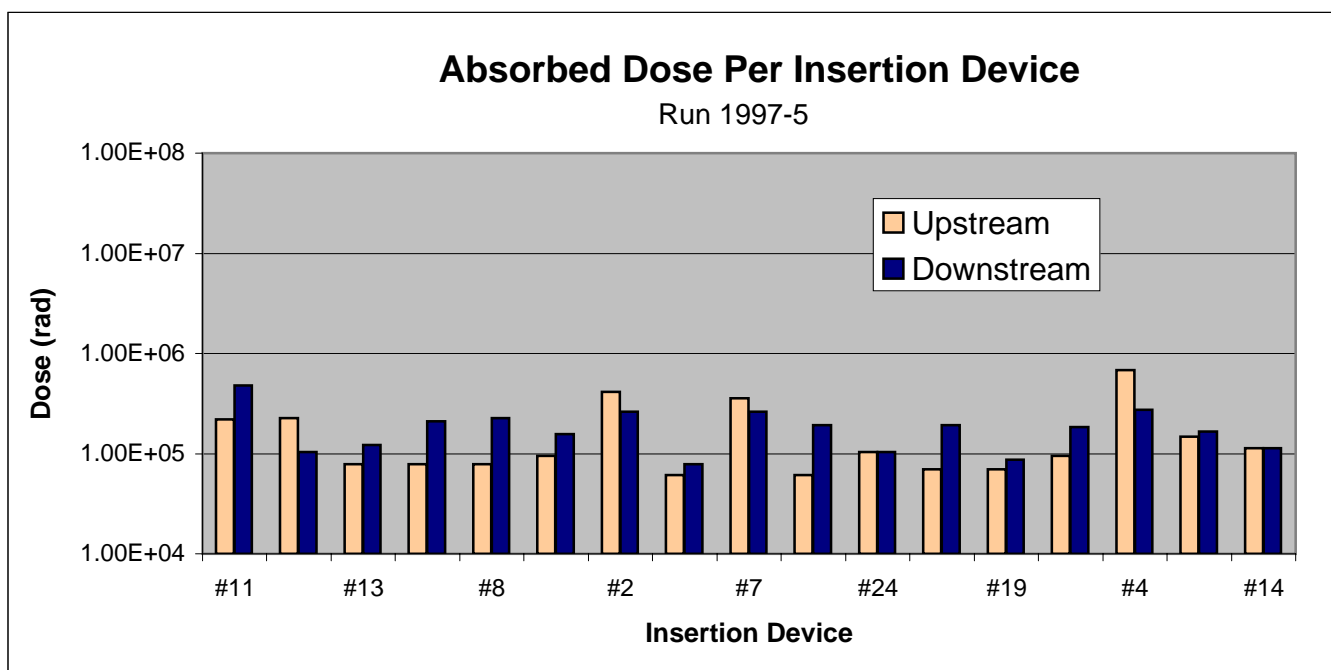
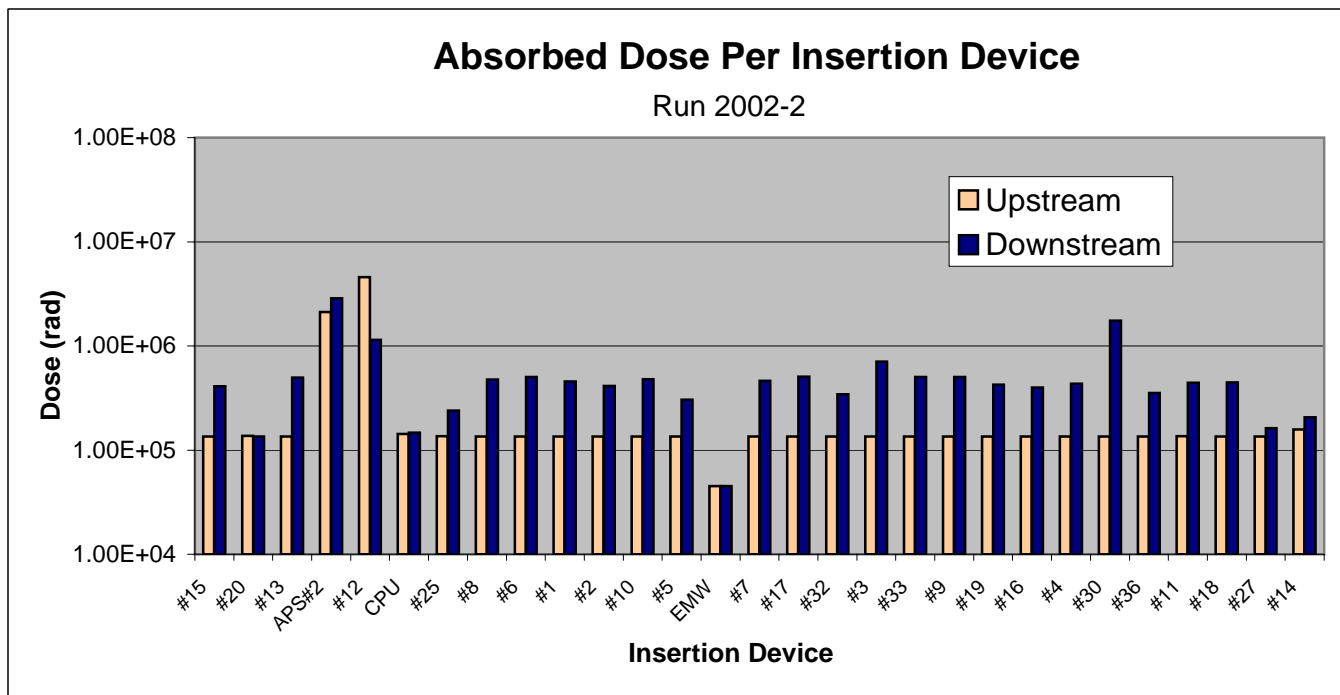**Figure 10: Measured Insertion Device Doses for Run 1997-5**
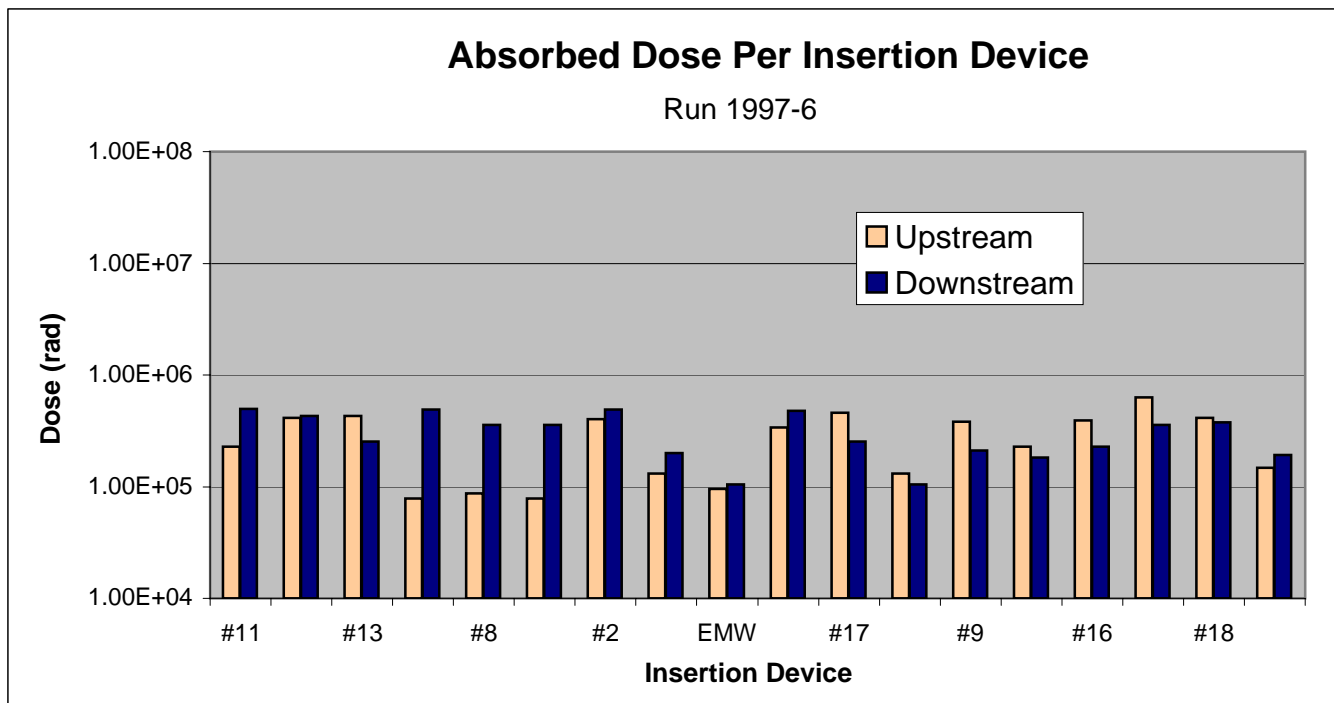
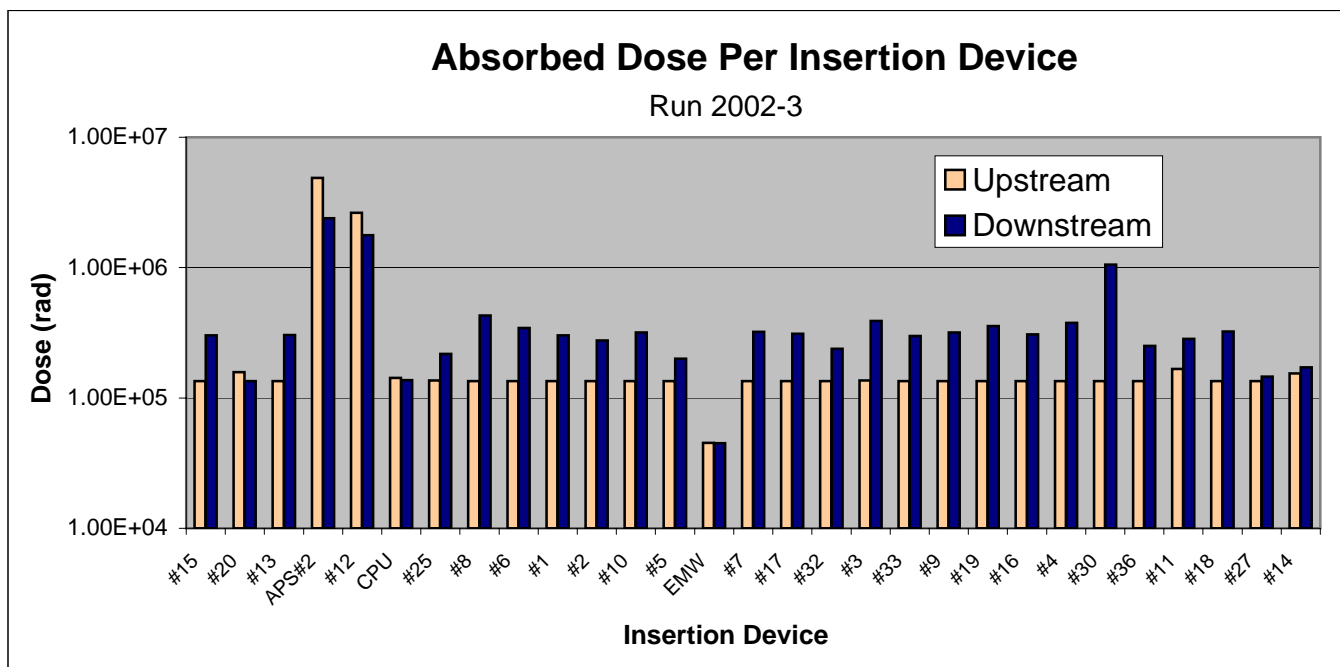**Figure 11: Measured Insertion Device Doses for Run 1997-6**
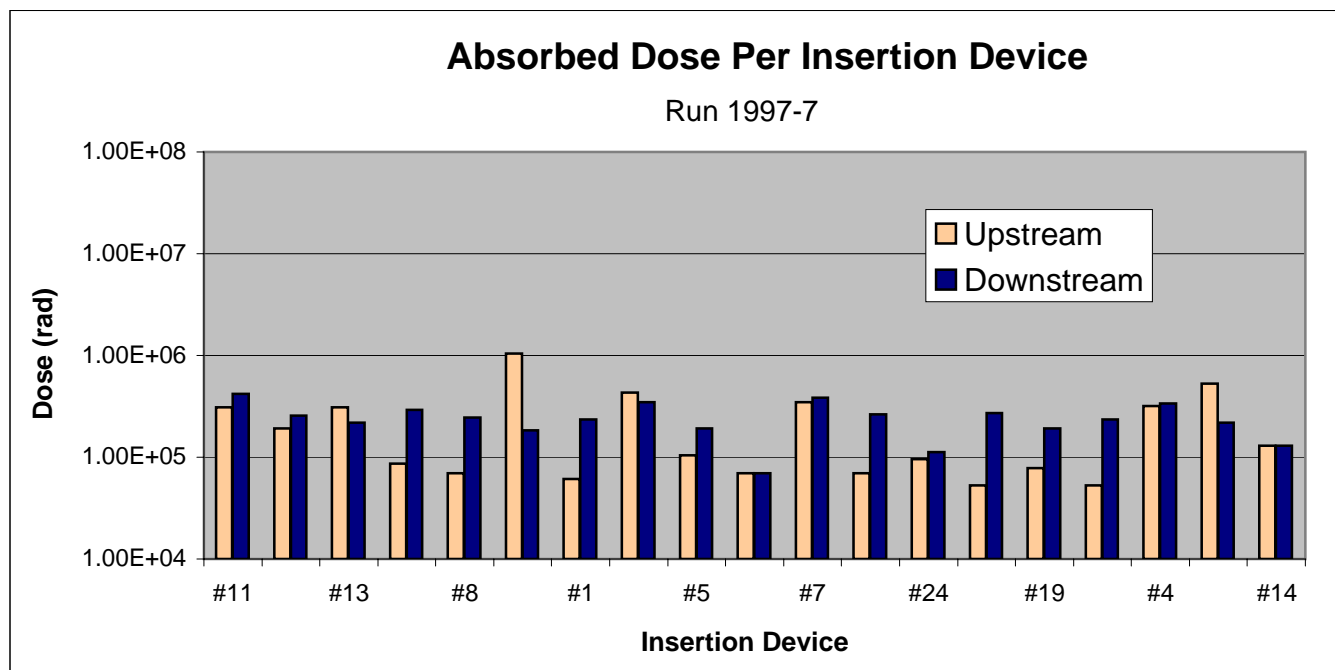
Figure 12: Measured Insertion Device Doses for Run 1997-7
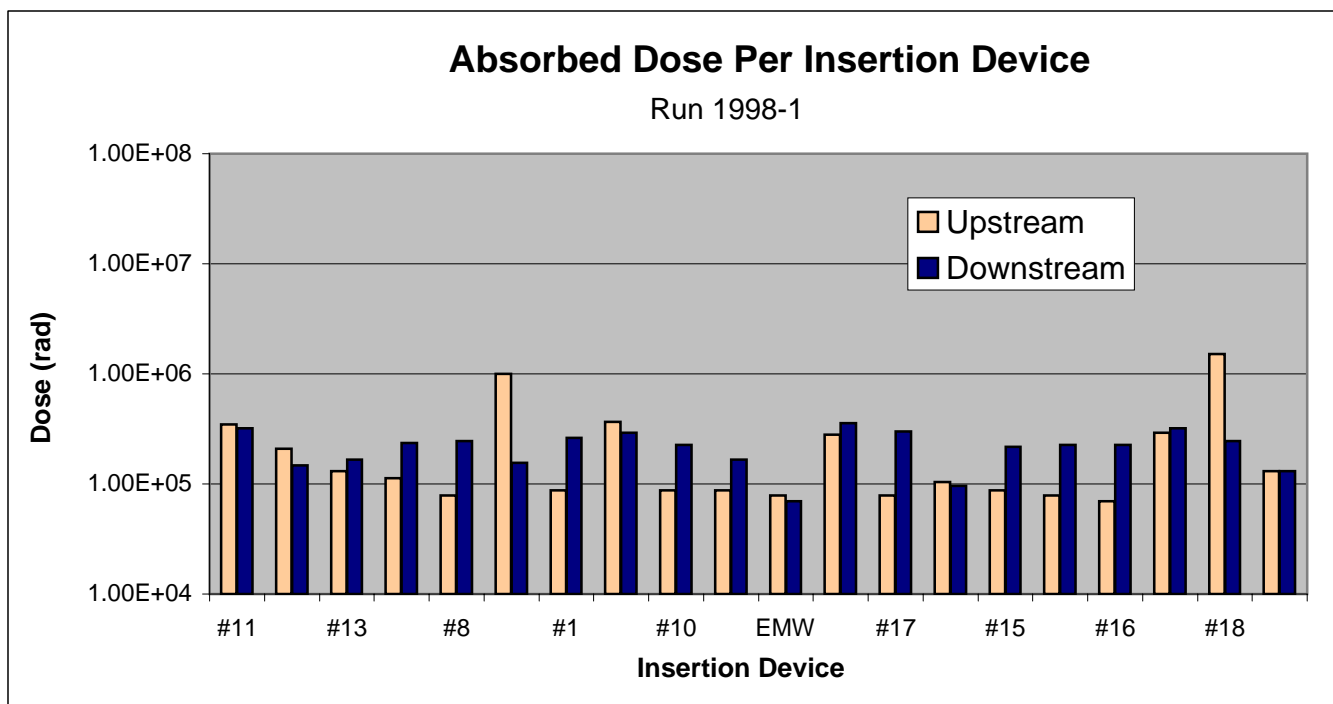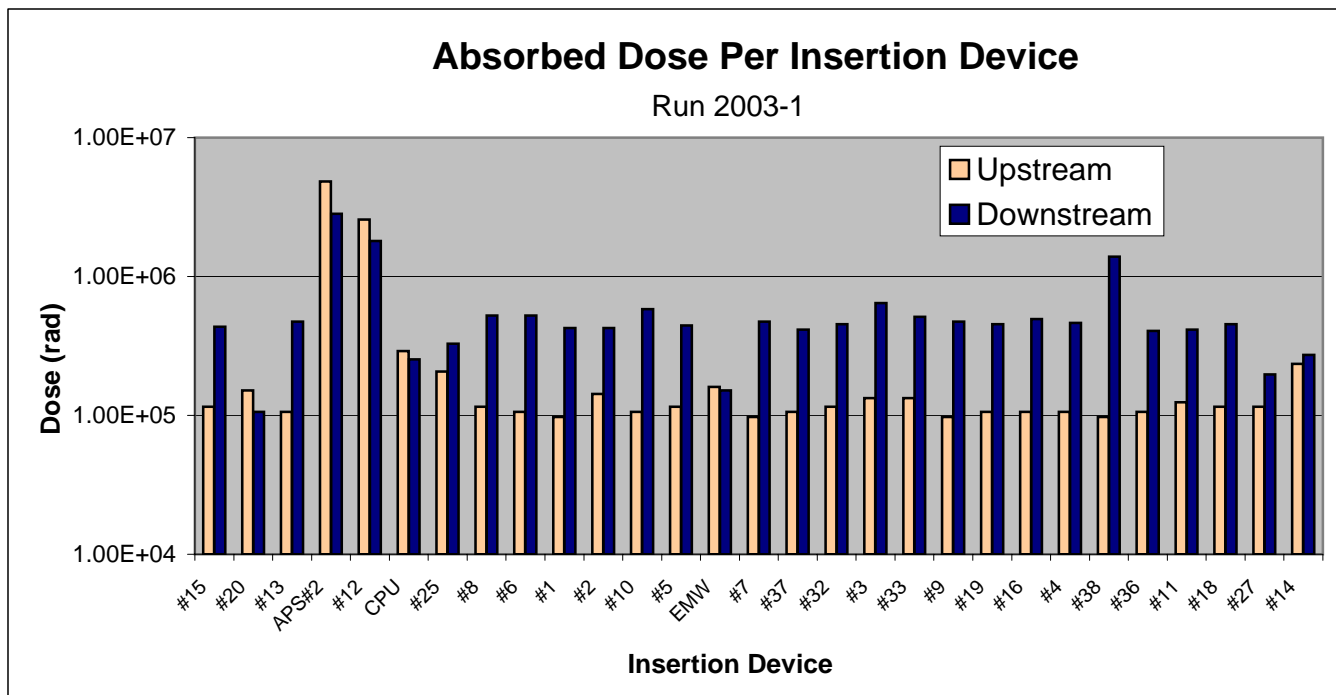
Figure 13: Measured Insertion Device Doses for Run 1998-1
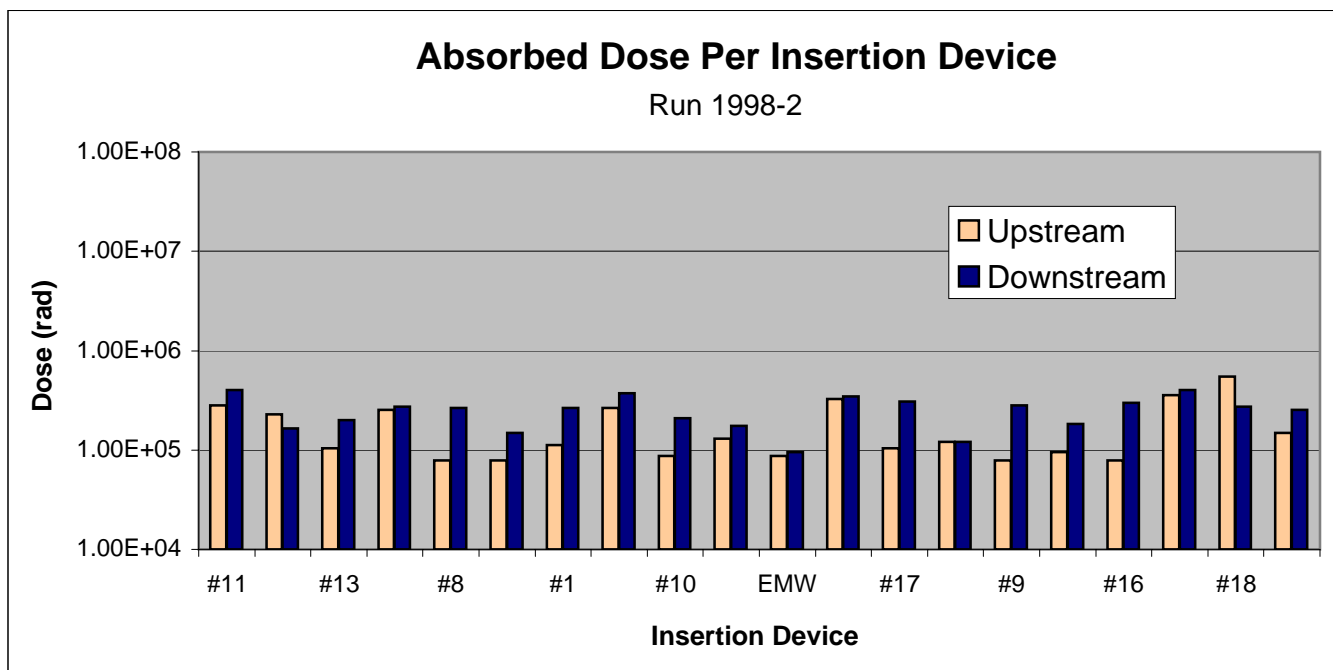
Figure 14: Measured Insertion Device Doses for Run 1998-2
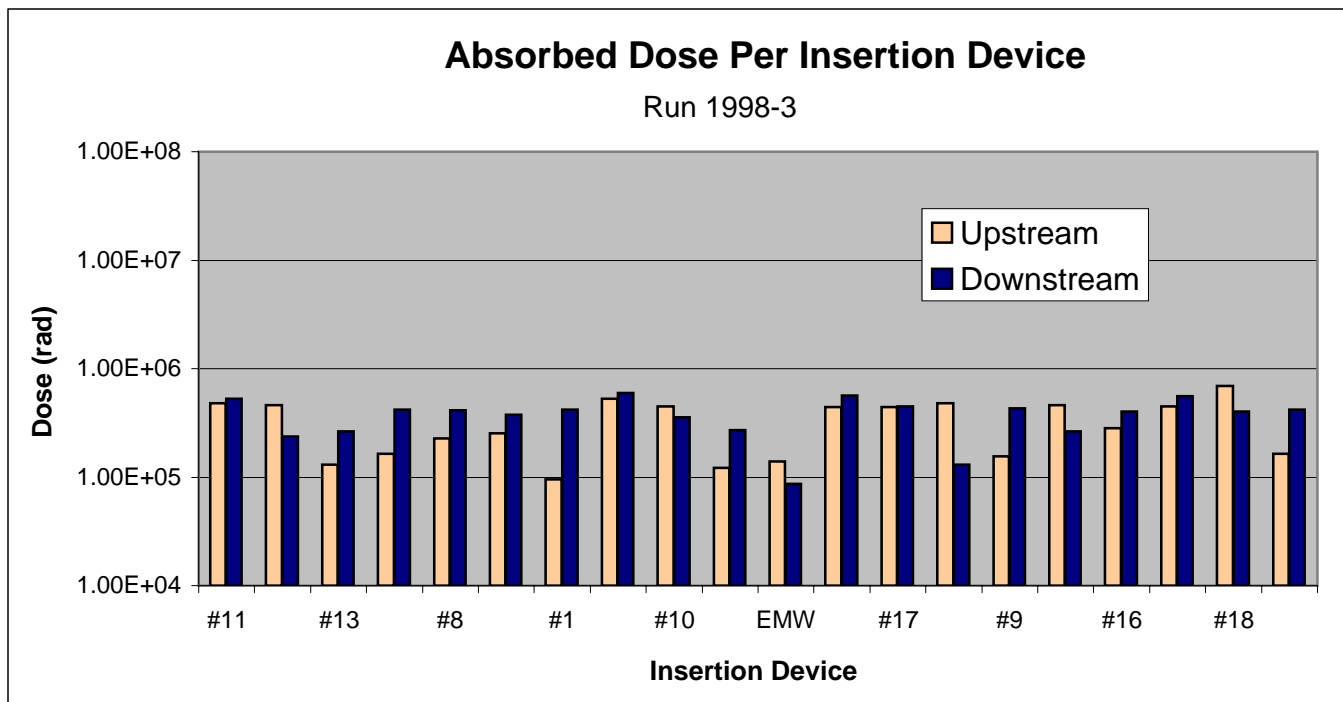
Figure 15: Measured Insertion Device Doses for Run 1998-3
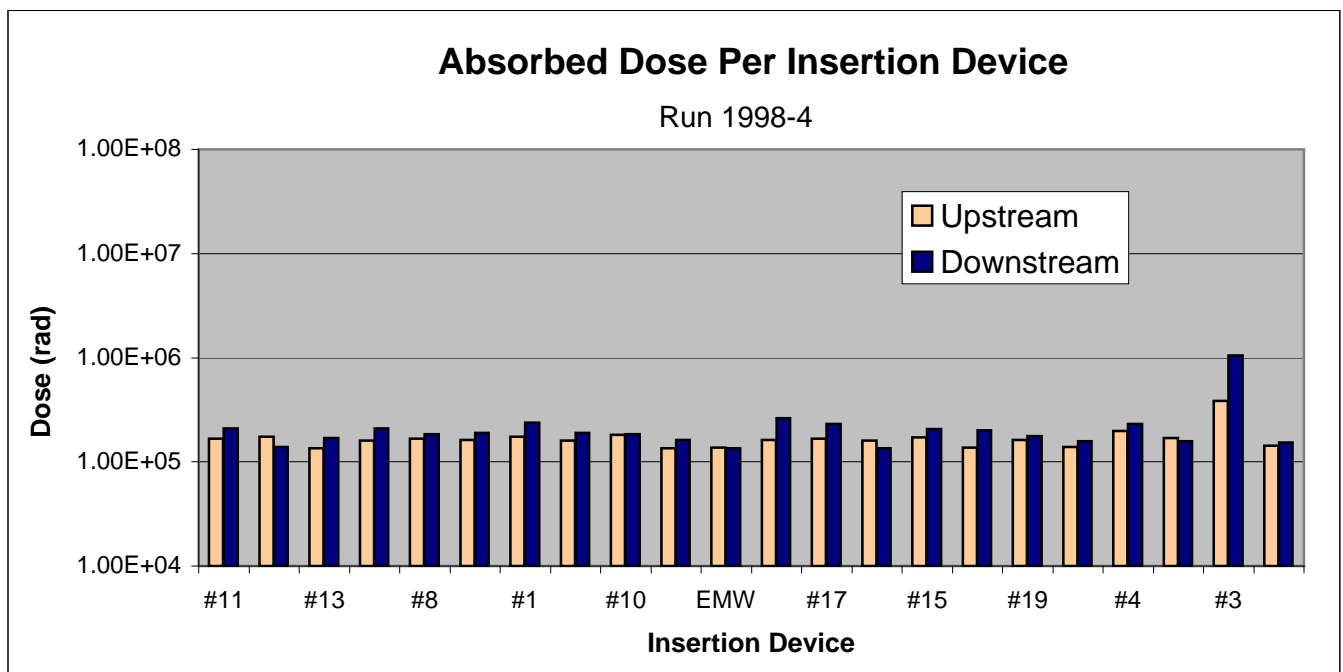
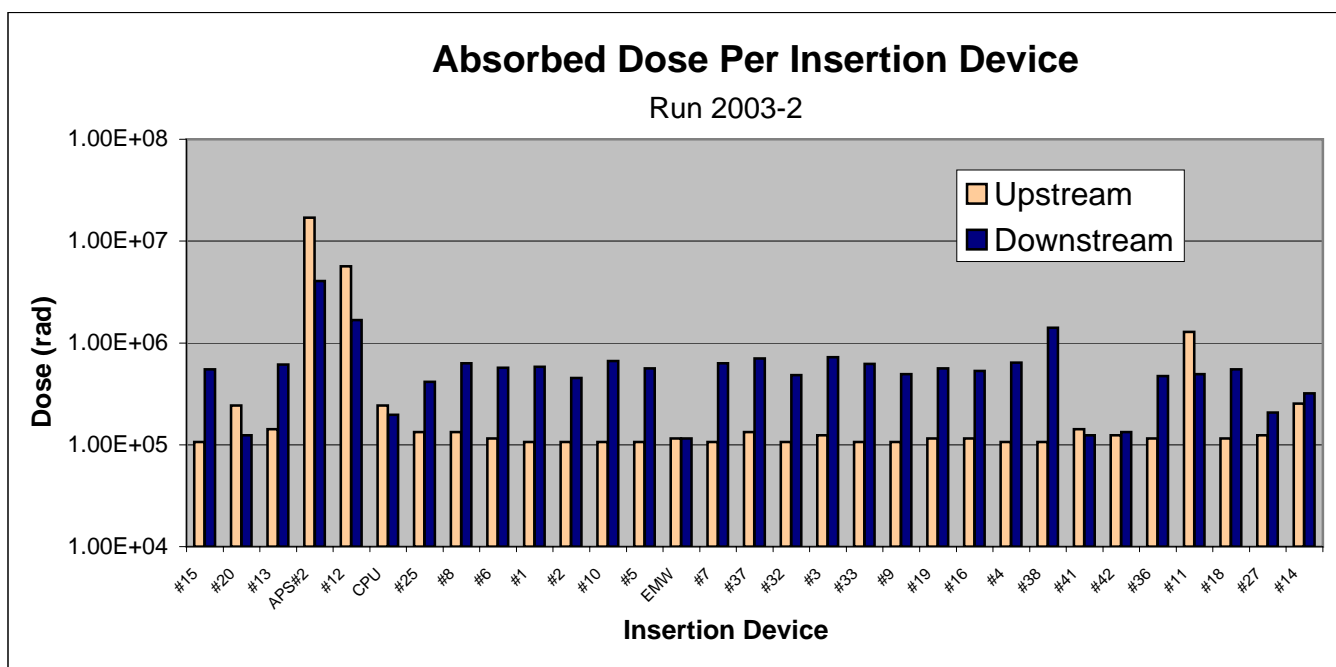**Figure 16: Measured Insertion Device Doses for Run 1998-4**
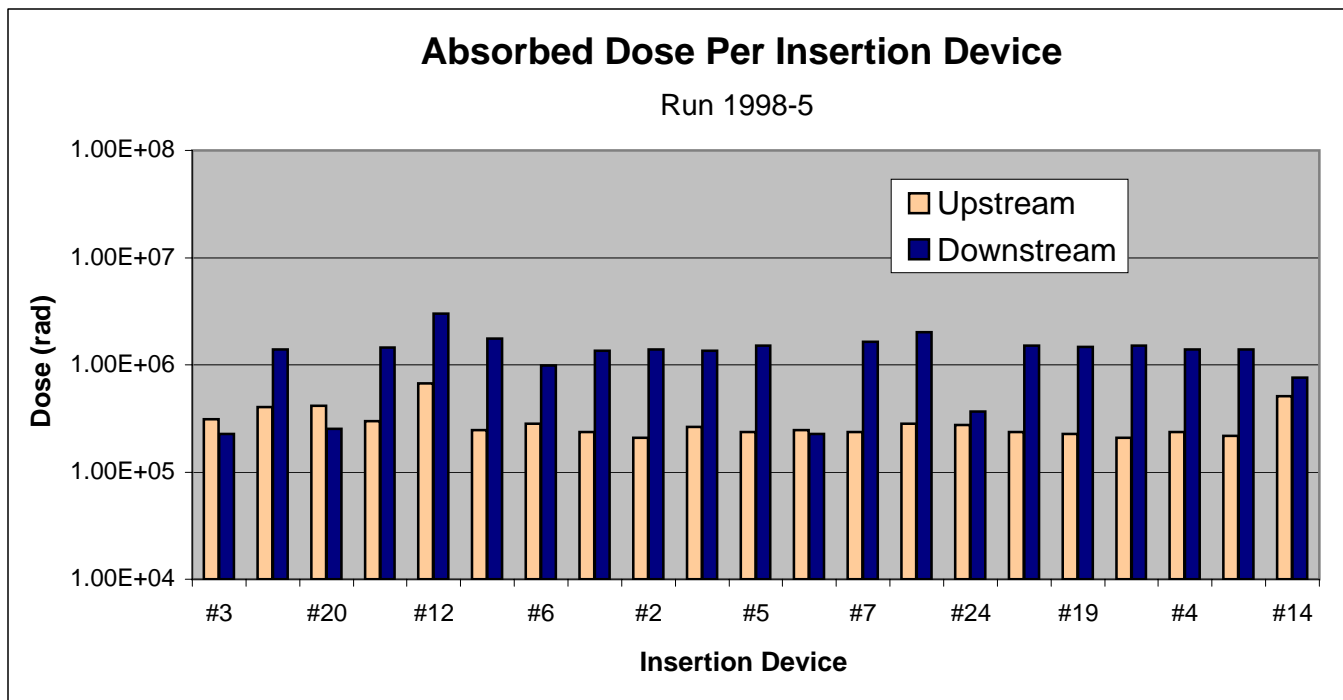
Figure 17: Measured Insertion Device Doses for Run 1998-5
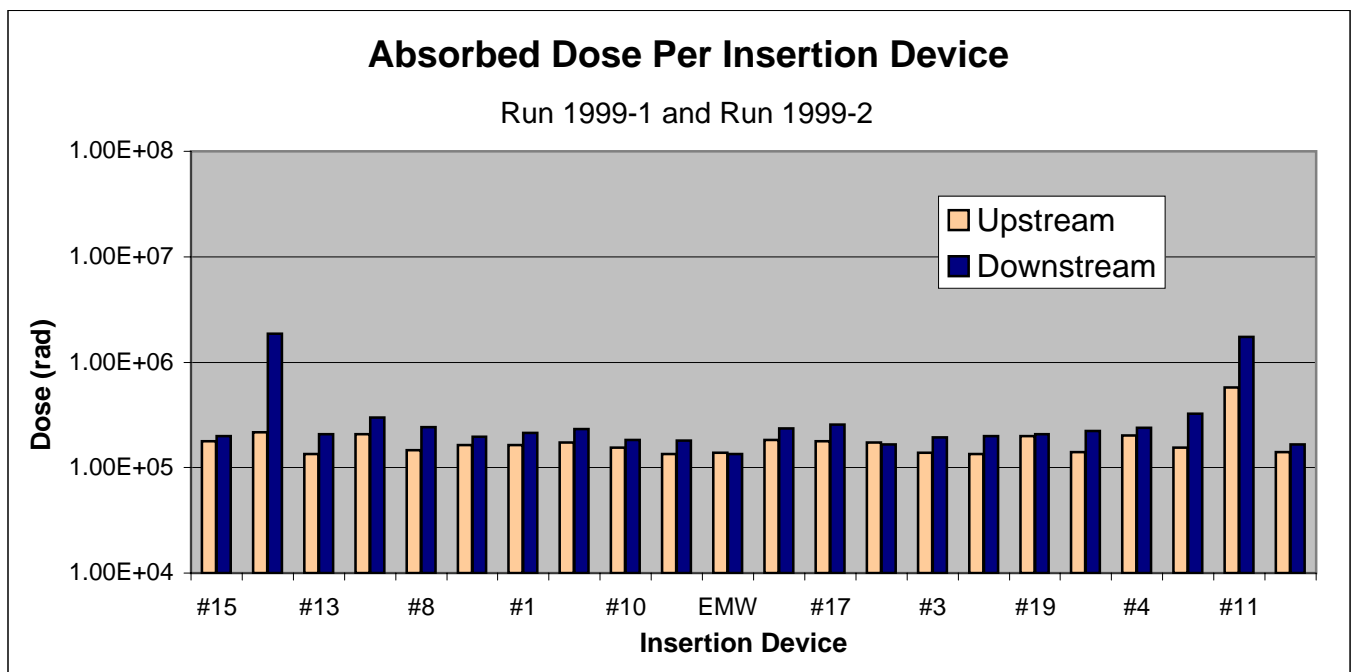
Figure 18: Measured Insertion Device Doses for Run 1999-1 and Run 1999-2
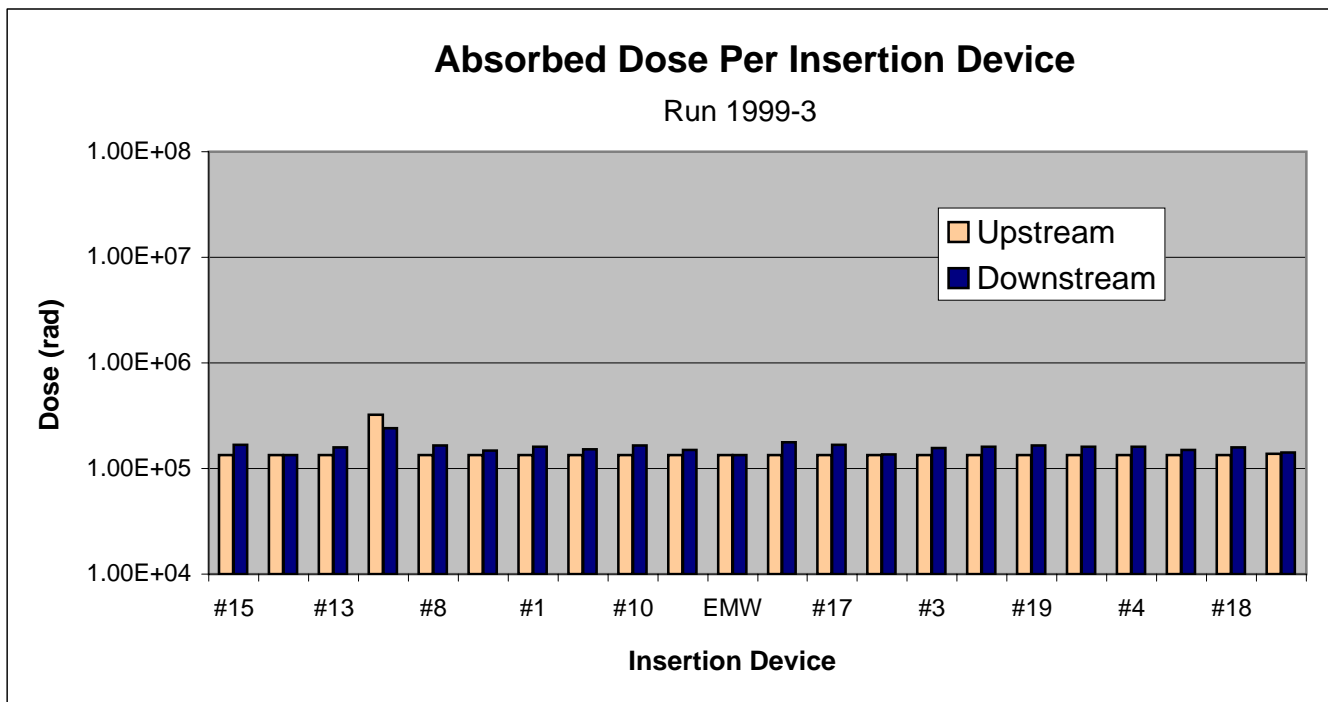
Figure 19: Measured Insertion Device Doses for Run 1999-3
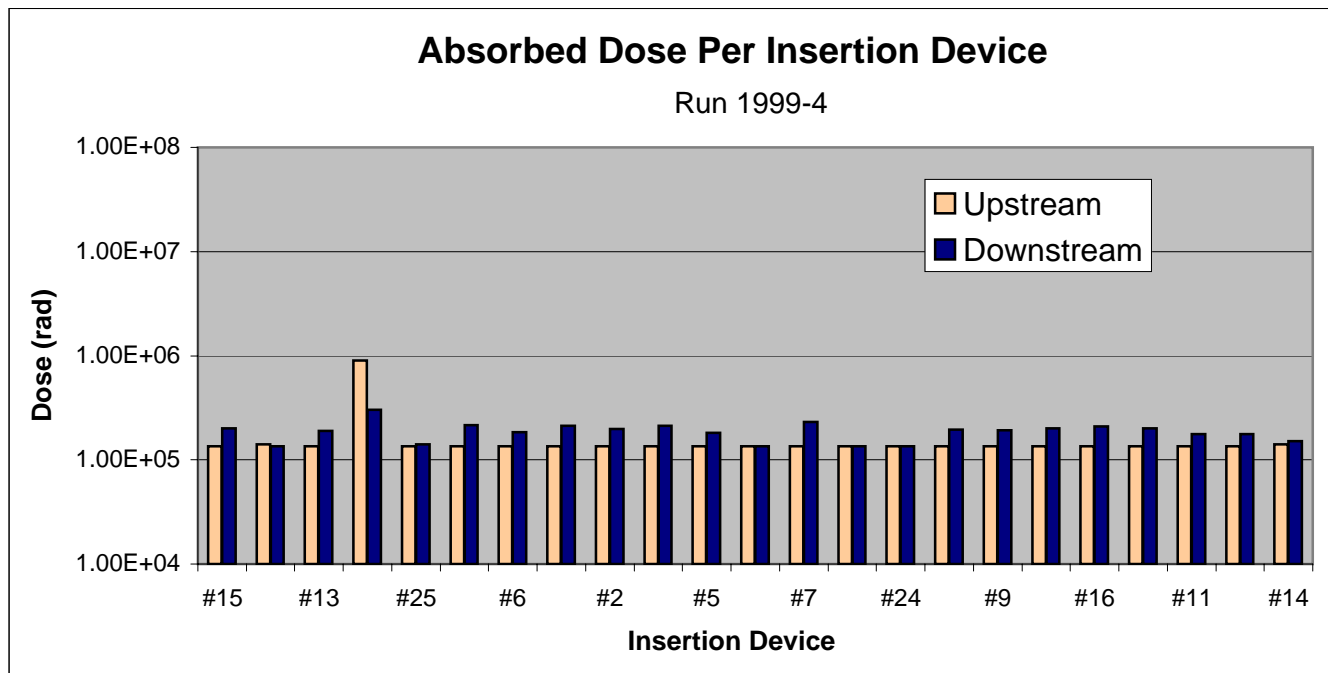
Figure 20: Measured Insertion Device Doses for Run 1999-4
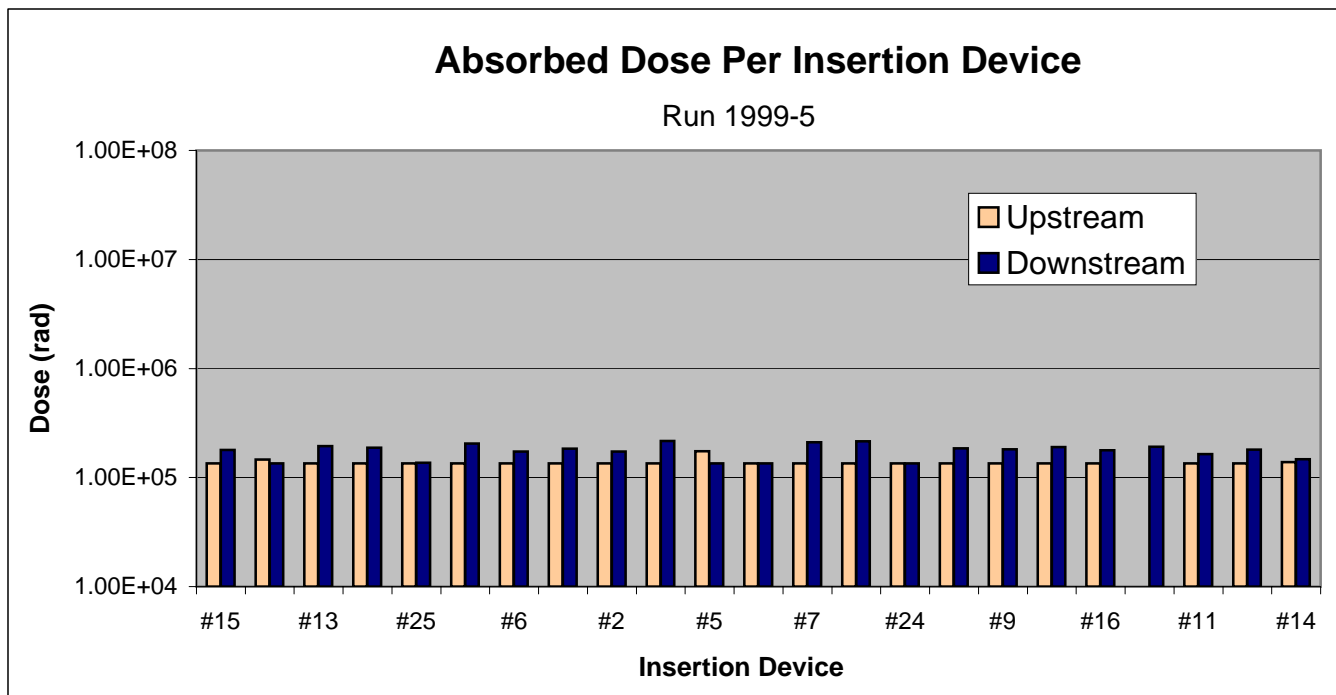
Figure 21: Measured Insertion Device Doses for Run 1999-5
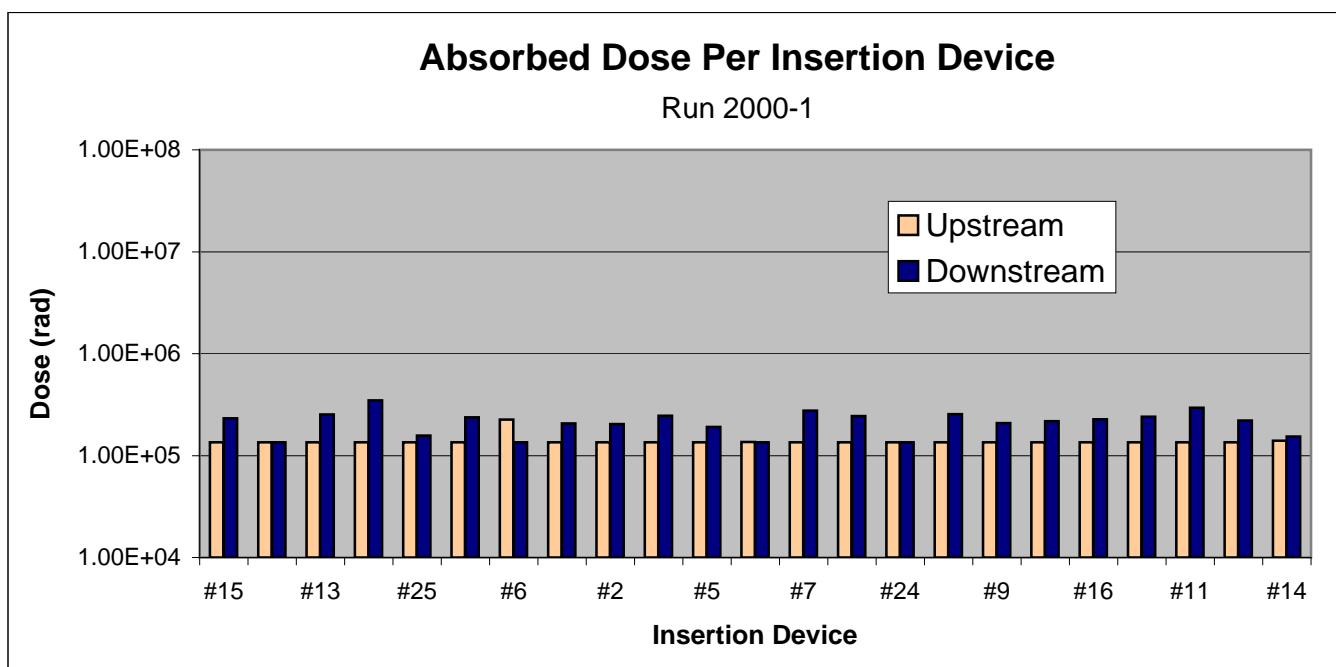
Figure 22: Measured Insertion Device Doses for Run 2000-1
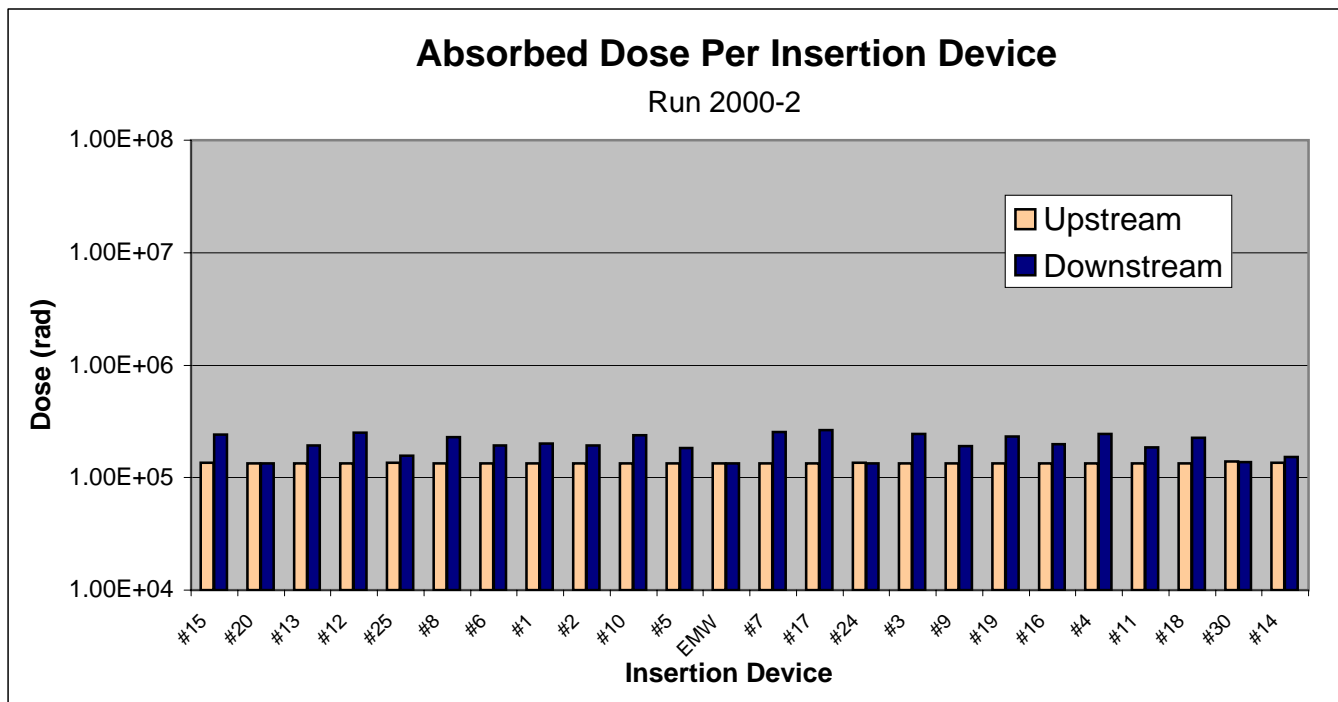
Figure 23: Measured Insertion Device Doses for Run 2000-2
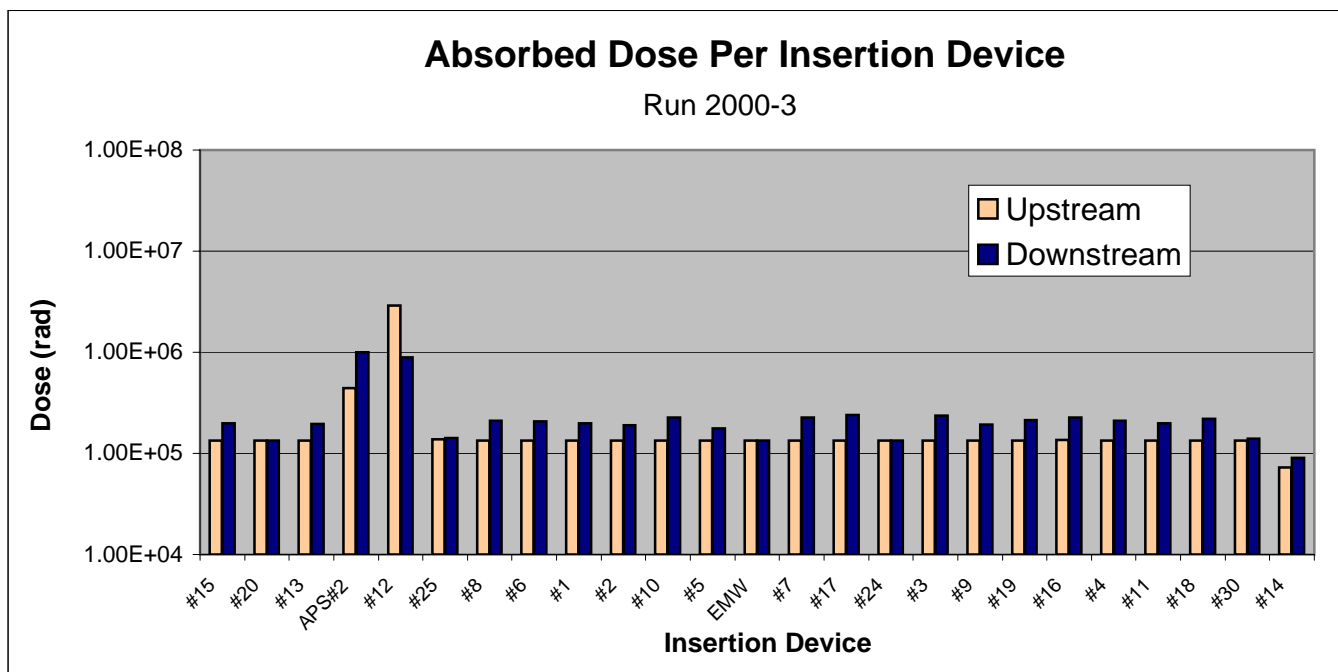
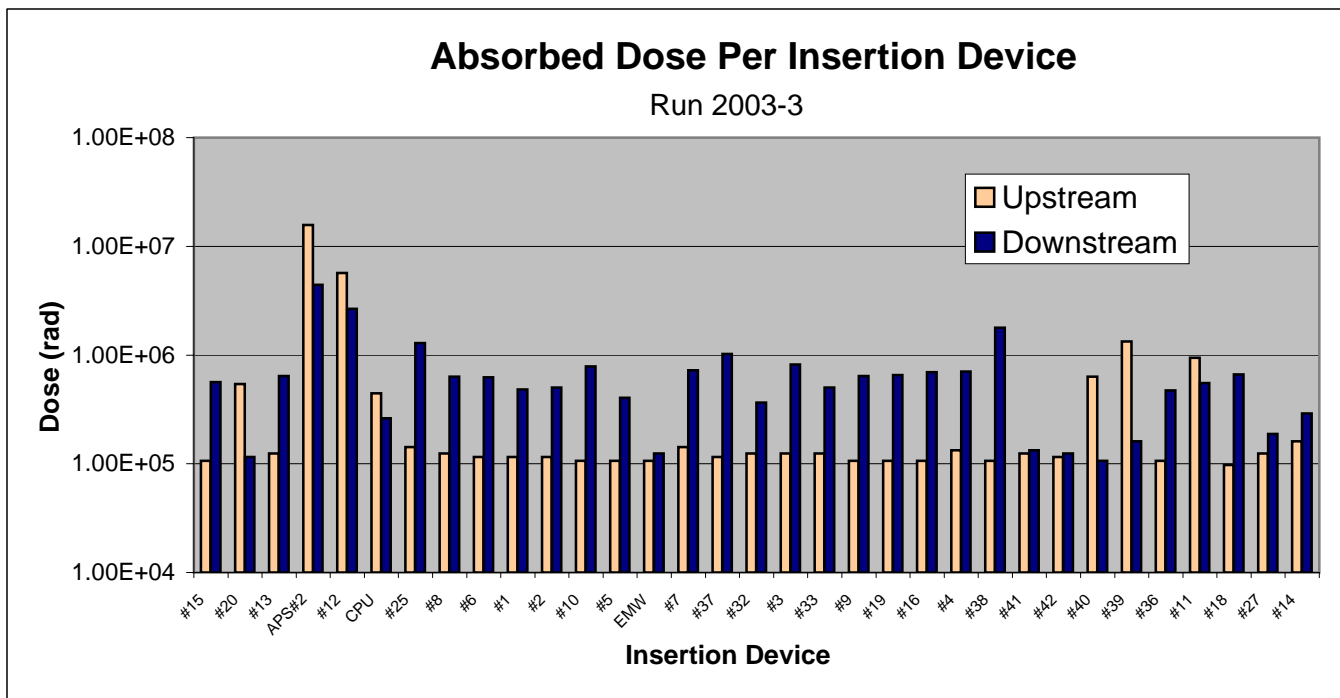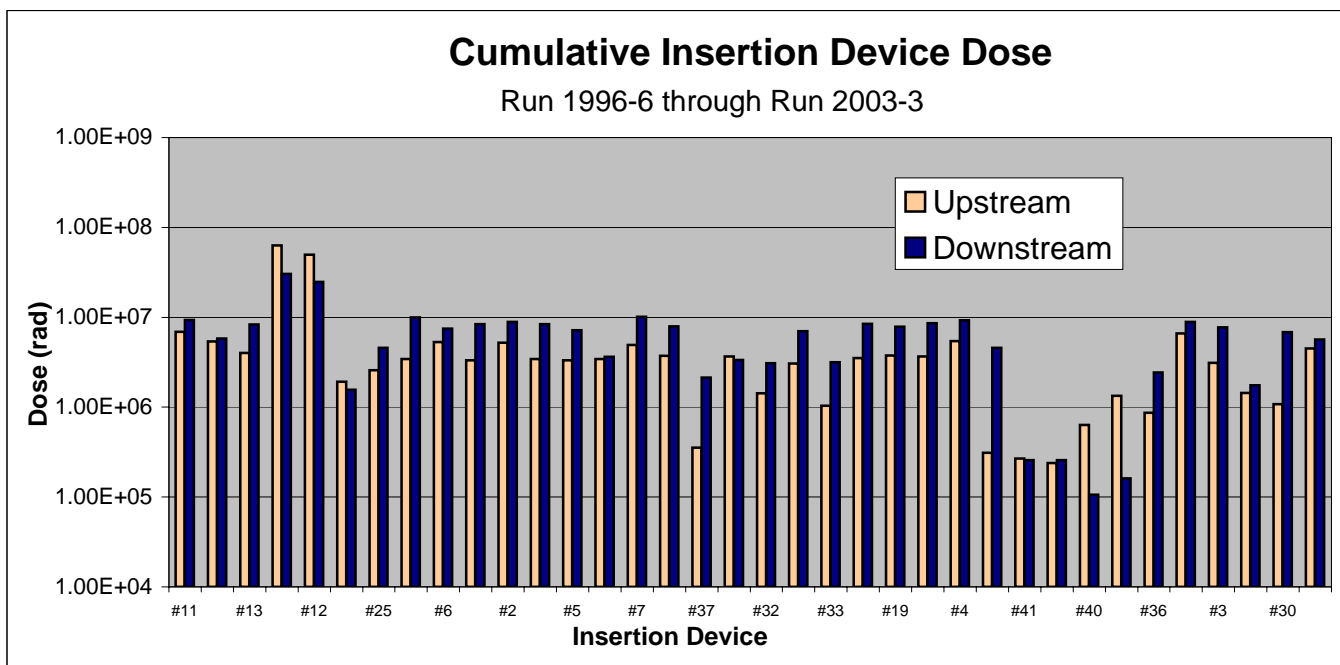**Figure 24: Measured Insertion Device Doses for Run 2000-3**
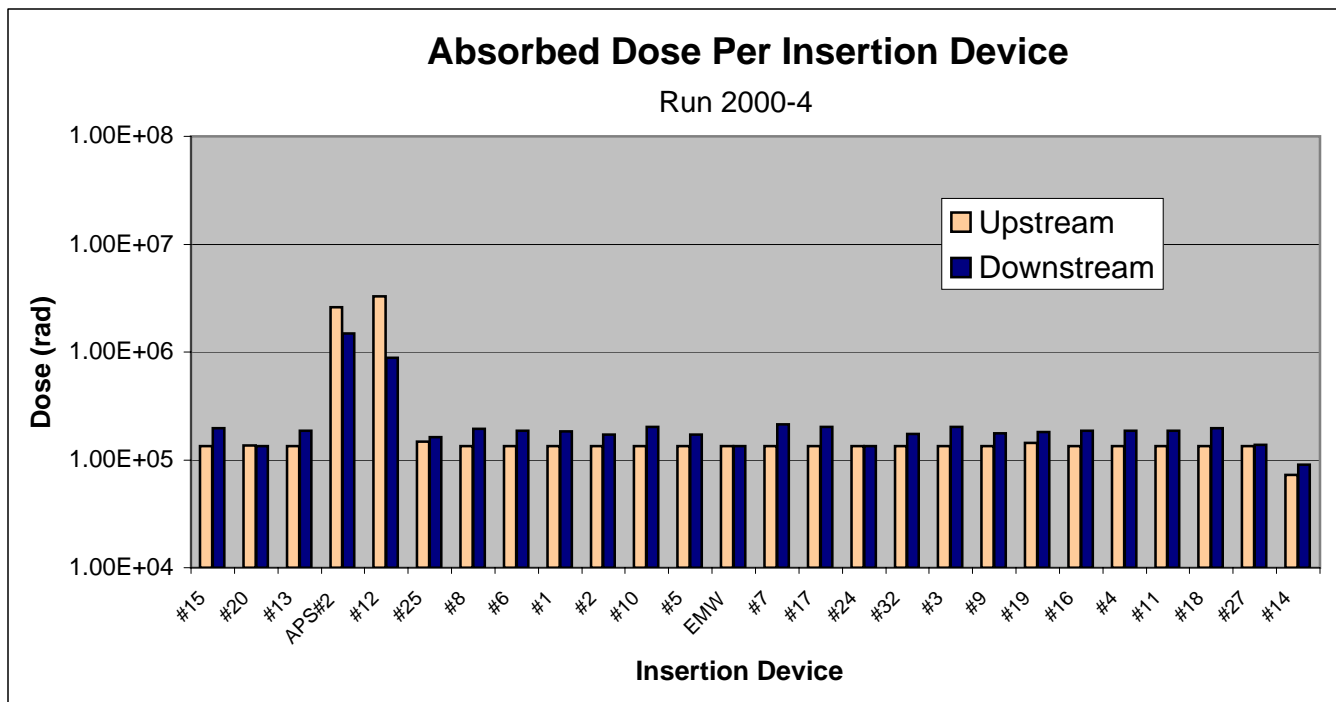
Figure 25: Measured Insertion Device Doses for Run 2000-4
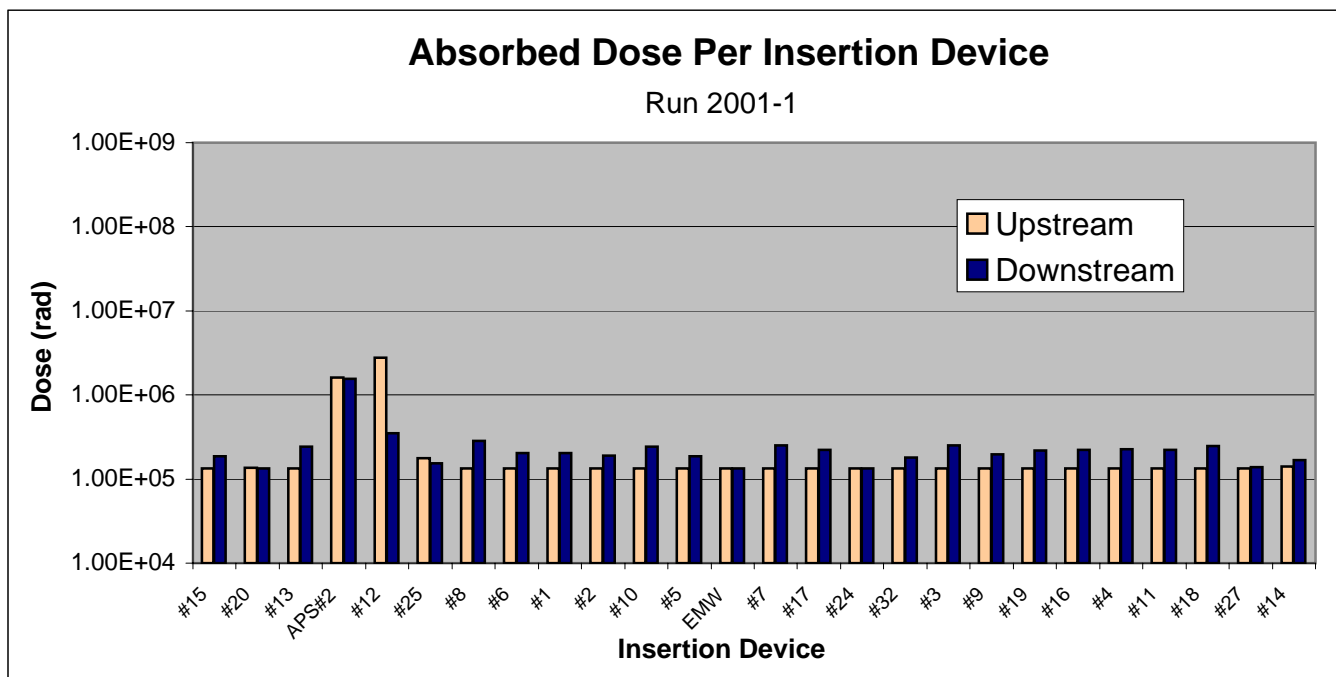
Figure 26: Measured Insertion Device Doses for Run 2001-1
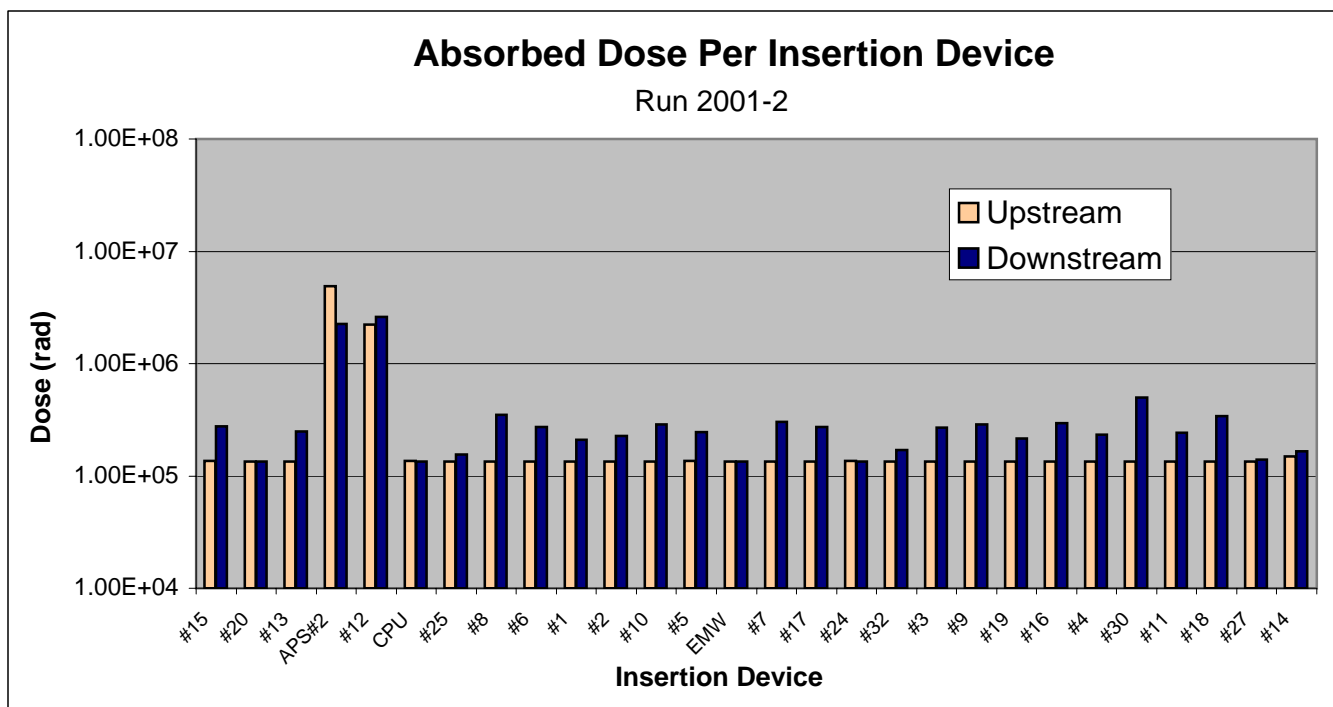
Figure 27: Measured Insertion Device Doses for Run 2001-2
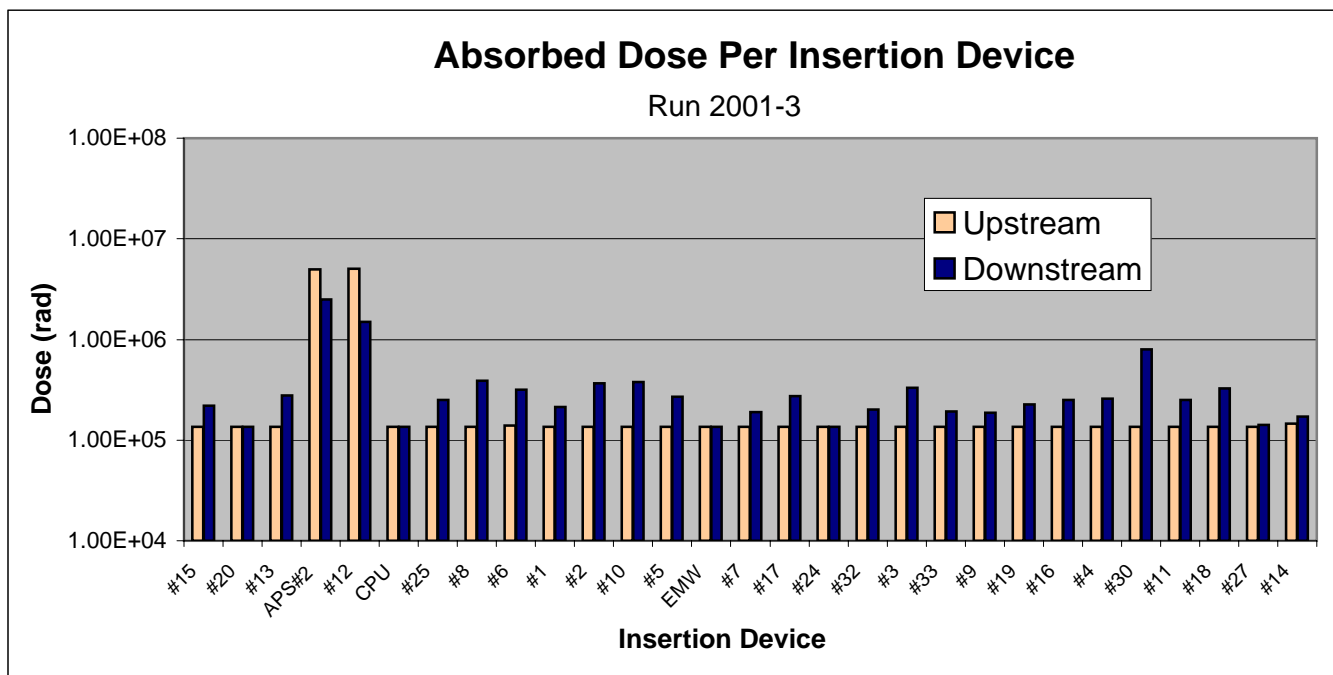
Figure 28: Measured Insertion Device Doses for Run 2001-3

Figure 29: Measured Insertion Device Doses for Run 2001-4

Figure 30: Measured Insertion Device Doses for Run 2002-1

Figure 31: Measured Insertion Device Doses for Run 2002-2

Figure 32: Measured Insertion Device Doses for Run 2002-3

Figure 33: Measured Insertion Device Doses for Run 2003-1

Figure 34: Measured Insertion Device Doses for Run 2003-2

Figure 35: Measured Insertion Device Doses for Run 2003-3

Figure 36: Cumulative Insertion Device Doses for Run 1996-6 through Run 2003-3
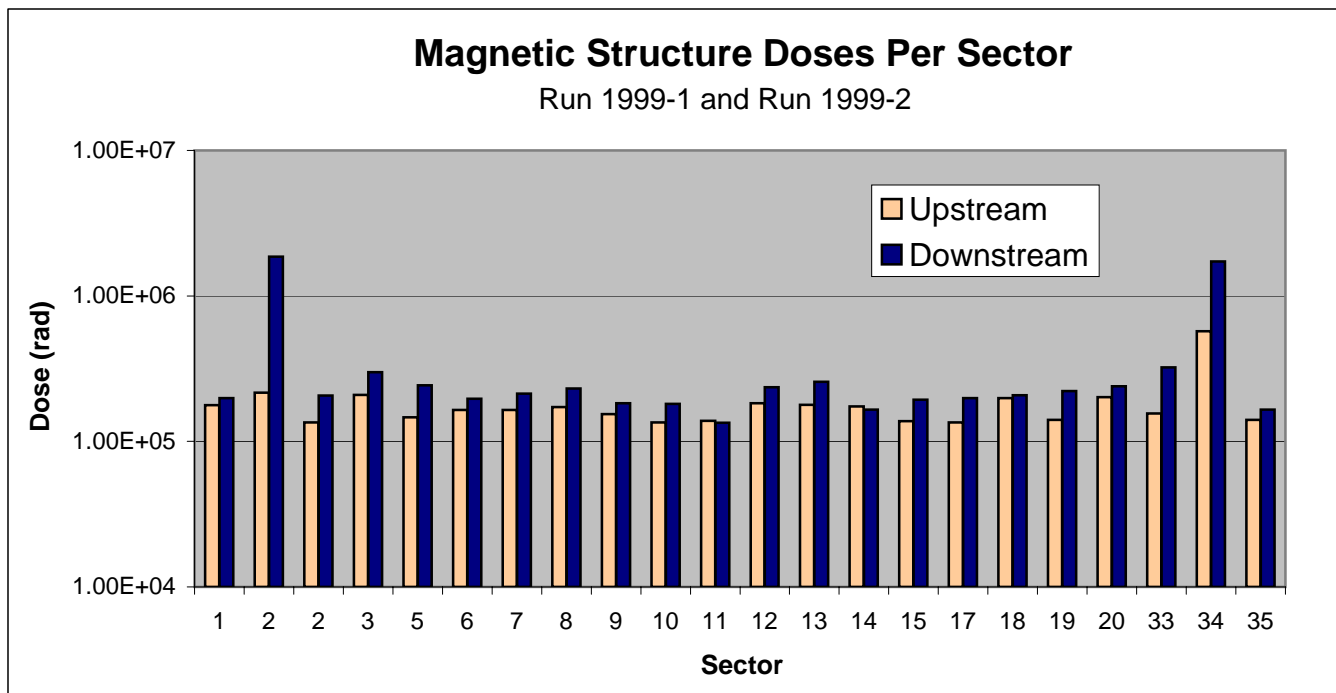
Figure 37: Measured Sector Doses for Run 1999-1 and Run 1999-2
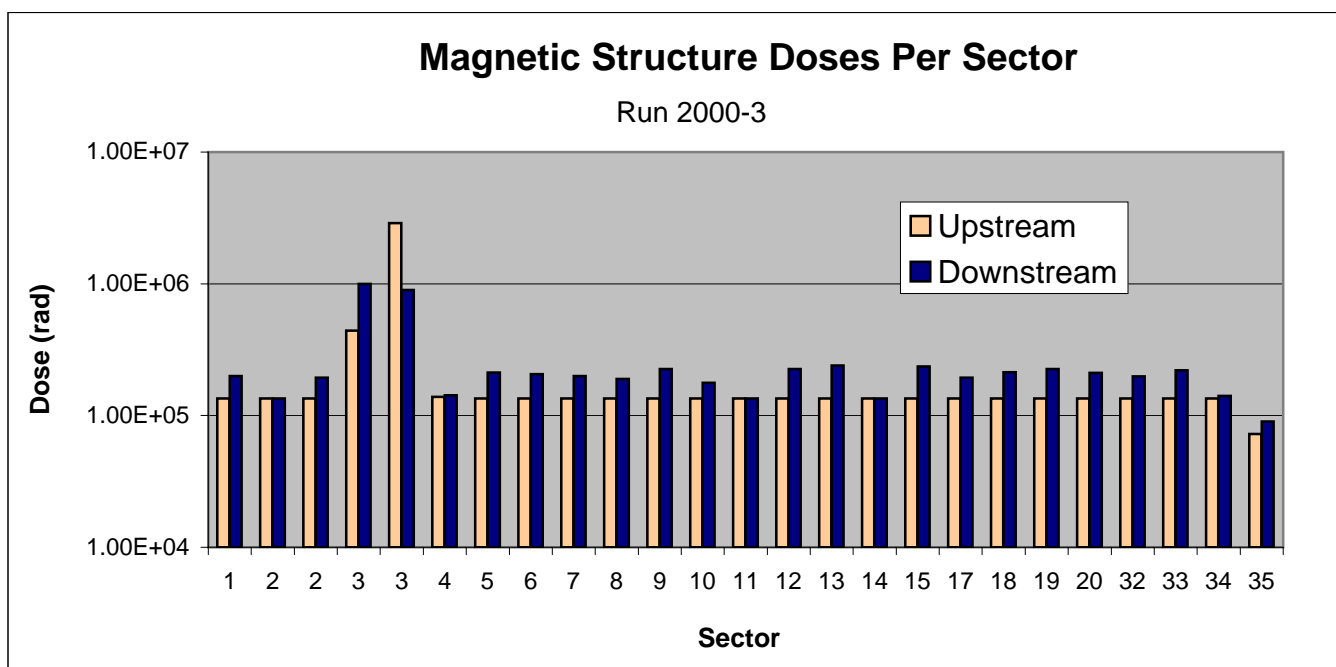
Figure 38: Measured Sector Doses for Run 2000-3
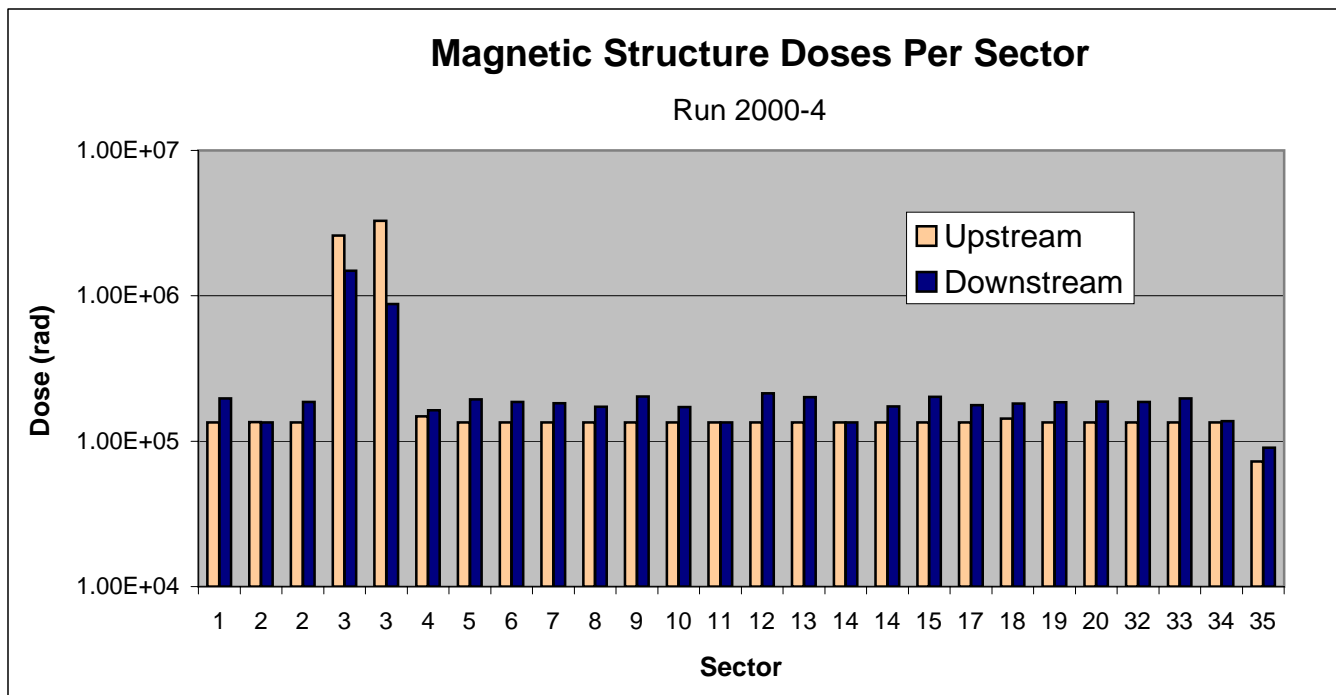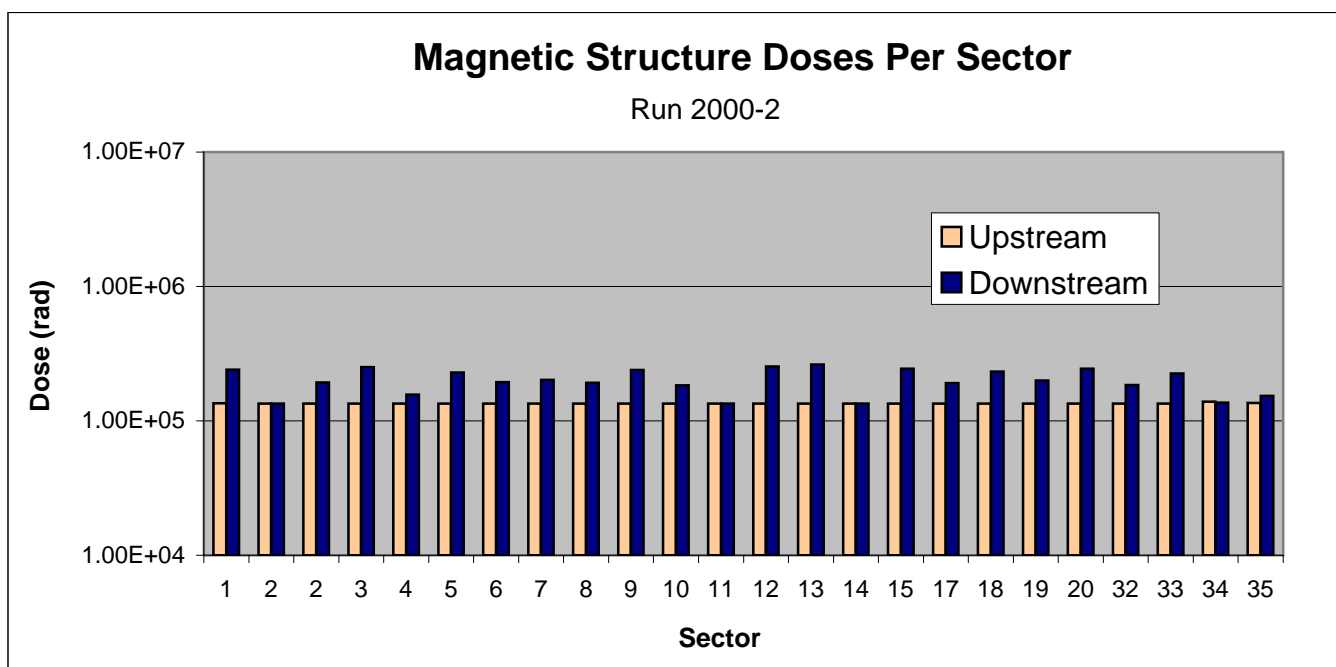
Figure 39: Measured Sector Doses for Run 2000-4

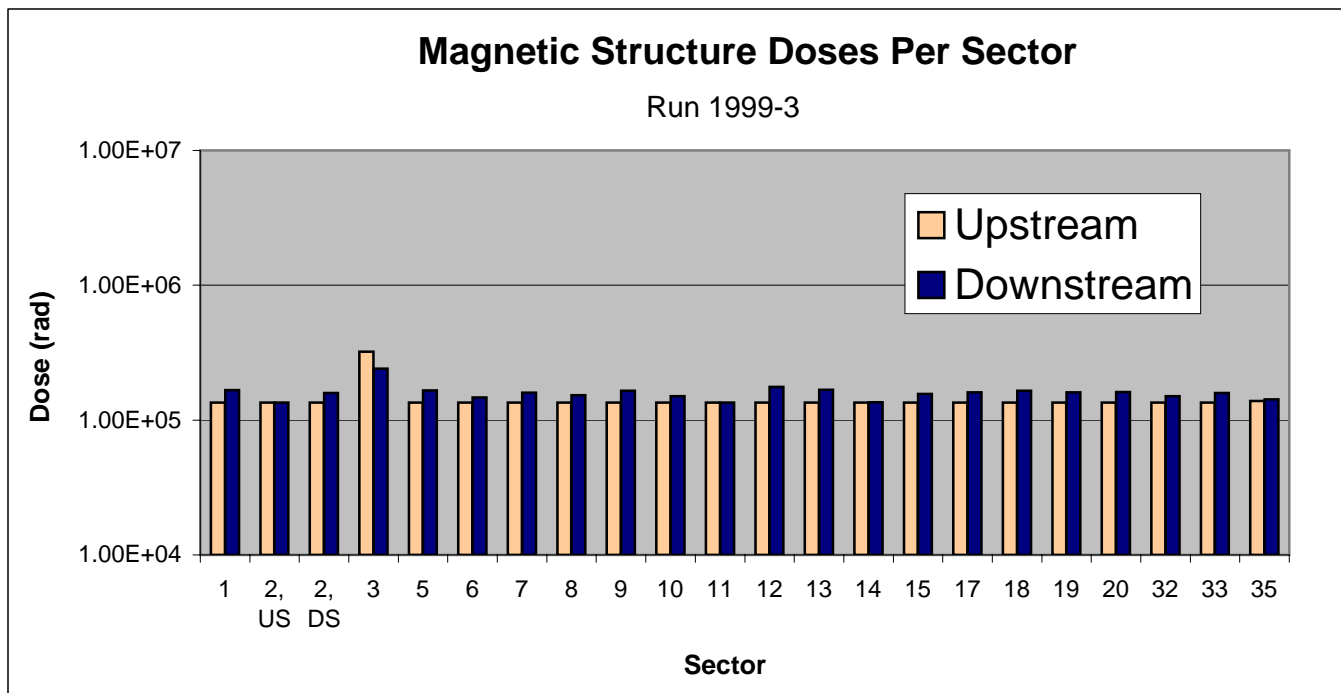**Figure 40: Measured Sector Doses for Run 2000-2**

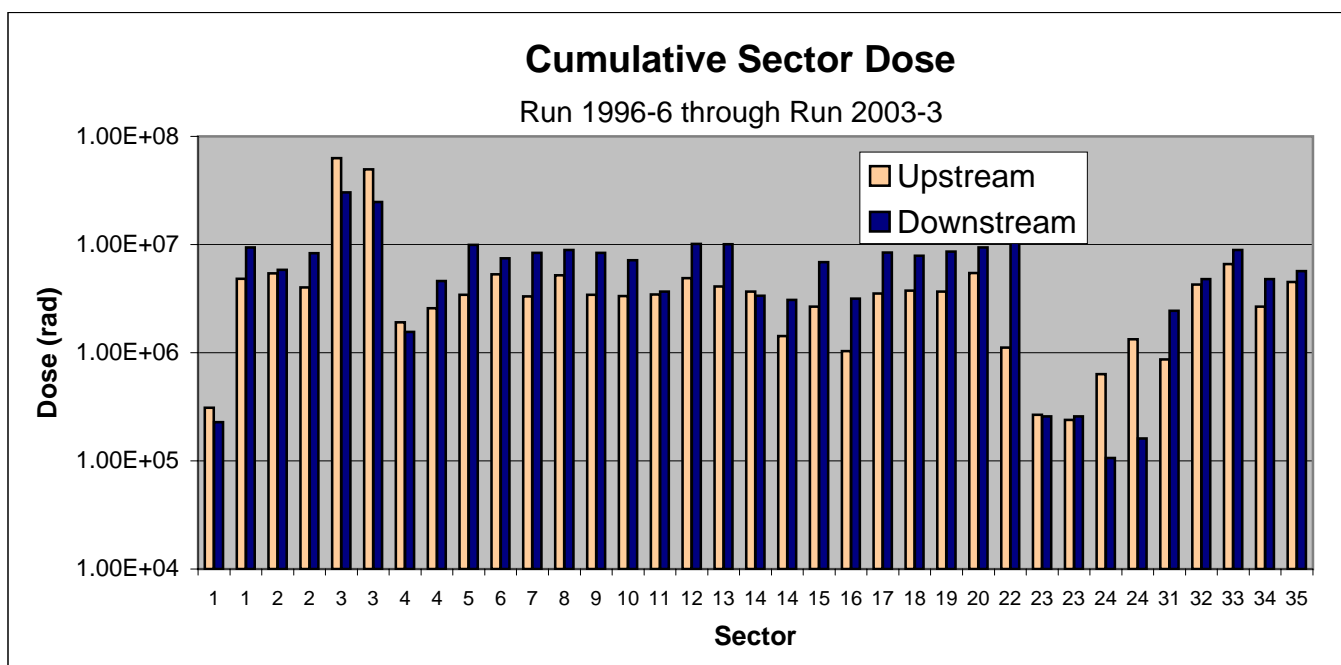**Figure 41: Measured Sector Doses for Run 1999-3**

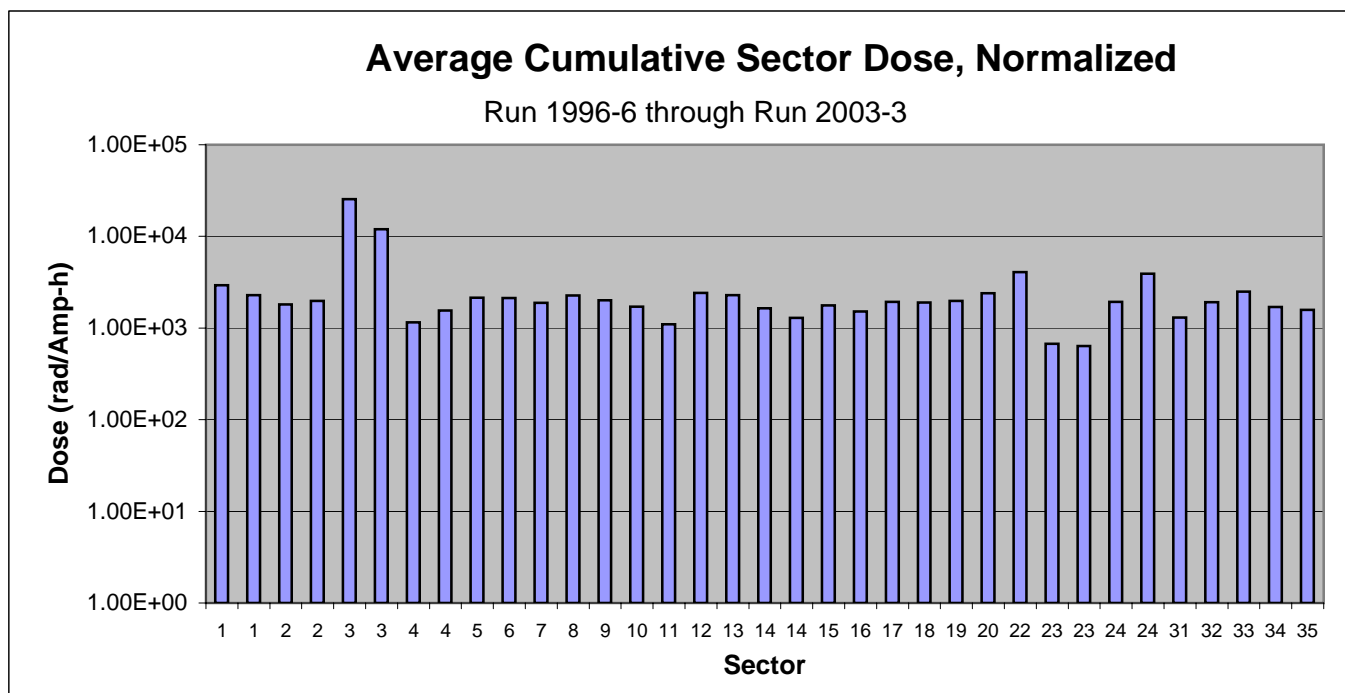**Figure 42: Cumulative Sector Doses for Run 1996-6 through Run 2003-3**

Figure 43: Average Cumulative Sector Doses for Run 1996-6 through Run 2003-3, Normalized